Monotone and stable residual distribution schemes on prismatic space-time elements for unsteady conservation laws

M. Mezine[+], M. Ricchiuto[*], R. Abgrall[+] and H. Deconinck[*]
[*] *von Karman Institute for Fluid Dynamics,*
Waterloosesteenweg 72, 1640 Sint-Genesius-Rode, Belgium
[+] *Mathématiques Appliquées de Bordeaux, Université de Bordeaux I,*
351 Cours de la Libération, 33405 Talence Cedex, France

Abstract

This paper is devoted to the construction of a class of stable, accurate and *compact* schemes for the solution of unsteady compressible flows equations on triangular unstructured meshes. We consider schemes of the Residual Distribution class. We first present a systematic way of constructing second order linear schemes for unsteady scalar advective problems. Then we consider the construction of non-linear monotone second order schemes. The approach is then extended to the system of the Euler equations. The approach is validated through well known scalar and Euler unsteady problems.

The schemes presented in the first part of the paper are monotone under a time-step restriction. In the last part of the paper we propose two approaches to overcome this limitation. Accuracy and robustness of the technique are proved on both scalar and Euler unsteady test-cases.

Contents

1 Introduction

This paper is devoted to the construction of a class of stable, accurate and *compact* schemes for the solution of unsteady compressible flows equations on triangular unstructured meshes.

In the past decades, many numerical methods have been applied to the simulation of unsteady compressible flows with discontinuities. In most cases, these methods are extensions of the so–called high order upwind schemes (see [1, 2] for a review), even on unstructured meshes [3]. There are at least two important exceptions to this, the finite element type schemes obtained with the stream–line diffusion method [4, 5] and the Discontinuous Galerkin schemes [6].

On unstructured meshes, the performances of the schemes constructed following the upwind high order philosophy are most of the times quite disappointing because of excessive numerical diffusion. To overcome this problem, one has resort to the ENO/WENO philosophy [7, 8]. Examples of such attempts are [9, 10, 8]. In these examples the price paid for the reduced numerical diffusion is very high : the coding is rather complex and moreover these schemes do not have a compact stencil, so their parallel implementation can be quite difficult. Besides, the analysis of the accuracy of the solution is rather unclear or at the least difficult to carry out.

In order to tackle these two problems – compactness of the stencil, effective analysis of the accuracy of the solution–, at least two classes of methods have emerged in the recent years: the Discontinuous Galerkin schemes (DG) and the Residual Distribution schemes (RD) or Fluctuation Splitting schemes. Though different in spirit, they have a common core at least in their "unstabilised" versions: the residual property. This property, discussed below in the framework of RD schemes, allows us to show the formal accuracy of the scheme on a very general mesh. The DG schemes use a discontinuous polynomial representation of the unknowns which is a generalization of what is done in finite volume schemes. The solution is updated via the evaluation of fluxes and the stabilization mechanism is obtained by very similar techniques to those in classical finite volumes. The net effect of this is to formally lose the residual property.

On the contrary, the RD schemes use a point-wise representation of the solution, as in finite difference schemes. The unknowns are updated by evaluation of the amount of the residual sent to the vertices and the stabilization mechanism can be similar to artificial viscosity, as in the SUPG finite element method [11] or the stream–line diffusion method [4], or inspired by the nonlinear techniques of the so–called high resolution schemes [12, 2]. One can also take into account the genuinely multidimensional nature of the problem [13].

In this paper, we consider schemes of the RD class, borrowing ideas from the upwind high order philosophy, as well as ideas coming from the stream–line diffusion one. Our goal is to propose a systematic construction of robust and high order schemes, on general meshes. This problem has received a lot of interest recently : one may quote the pioneering work of Roe, Sidilkover, Deconinck and their coworkers [14, 15, 13] and also more recently in [16, 17, 18], but only for *steady* problems. Here we consider unsteady problems. The present paper contains to a large extent the material published by Abgrall and Mezine in the early draft that has been presented in the second AMIF conference, October 2000 [19]. However, here we will report a more general and detailed analysis of the approach and more recent results as well. Independently, other schemes for unsteady systems have also been recently constructed by different authors [20, 21, 22, 23] but these schemes are either *a priory* computationally more demanding or they are not monotonicity preserving in general.

The paper is organized as follows. First, we recall some basic facts about upwind residual distribution schemes. Then we show how to construct, for scalar problems, a class of upwind, monotonicity preserving and second order schemes. Several numerical examples are considered to show the effectiveness of the approach. Then we extend this method, following the ideas of [24], first to symmetrizable systems, then to the Euler equations. The main drawback of this class of schemes is that monotonicity (but not stability) is guaranteed under a time-step constraint, similar to the CFL condition. To overcome this limitation, first, following an idea of Csik *et al.* [23], we construct an unconditionally stable, monotonicity preserving and second order accurate scheme for unsteady flow problems which works on three time levels. We then present an alternative solution borrowing from the recent work of Abgrall and Roe on very high order schemes [25] the idea of the use of an *inconsistent* low order scheme in the construction of a non-linear positive high order one. Throughout the paper we show several numerical examples to illustrate our technique. Some conclusions and remarks for future developments end the paper.

2 Petrov-Galerkin formulation of Residual Distribution approach

We will consider for the moment the solution of the following scalar problem:

$$\overrightarrow{\lambda} \cdot \nabla u = \left\langle \overrightarrow{\lambda}, \nabla u \right\rangle = 0 \text{ in } \Omega \tag{1}$$

with $\overrightarrow{\lambda}$ constant. On a given triangulation τ_h of Ω, the Residual Distribution schemes can be viewed as a class of Petrov-Galerkin finite element schemes. In order to show it we start by writing the RD discrete version of equation (1) for a generic node $M_i \in \tau_h$:

$$\sum_{T, M_i \in T} \Phi_i^T = \sum_{T, M_i \in T} \beta_i^T \Phi^T = 0.$$

In last equation we have denoted with $\beta_i^T = \Phi_i^T / \Phi^T$ the distribution coefficients and with Φ^T the residual defined by

$$\Phi^T = \int_T \left\langle \overrightarrow{\lambda}, \nabla u^h \right\rangle \, dx$$

Denoting by $\mathcal{N}_i$ the linear finite elements shape function and with w_i the Petrov-Galerkin weighting function associated to node i defined by:

$$w_i = \mathcal{N}_i + \alpha_i^T \text{ on } T$$

with α_i^T constant, one can choose α_i^T such that the spatial discretization of the Petrov-Galerkin formulation is the same as the Residual Distribution approach. Starting from the finite element spatial discretization of (1)

$$\sum_{T \in \tau_h} \int_T w_i \left\langle \overrightarrow{\lambda}, \nabla u^h \right\rangle \, dx = 0. \tag{2}$$

Since $\left\langle \overrightarrow{\lambda}, \nabla u^h \right\rangle$ is constant on T and equal to $\Phi^T / |T|$ one obtains

$$\sum_{T,M_i\in T}\int_T w_i\,dx\,\frac{\Phi^T}{|T|}=0. \tag{3}$$

Using the definition of w_i in the second integral in equation (3) leads to

$$\sum_{T,M_i\in T}(\frac{1}{3}+\alpha_i^T)\Phi^T=0. \tag{4}$$

Setting $\alpha_i^T=\Phi_i^T/\Phi^T-1/3=\beta_i^T-1/3$, the spatial discretization of the Petrov-Galerkin formulation is the same as that of the Residual Distribution approach.

We remark that this is not the unique way of formulating Residual Distribution schemes as Petrov-Galerkin schemes. An alternative way of doing it is to test equation (1) with a function belonging to the space of piecewise constant polynomials, namely we could choose

$$\tilde{w}_i=\sum_{T,M_i\in T}\chi_T\tilde{\alpha}_i^T,\quad \chi_T=1\ \text{ if } x\in T\ \chi_T=0\ \text{ otherwise}$$

Proceeding as before we obtain the finite element discretization

$$\sum_{T\in\tau_h}\int_T\tilde{w}_i\left\langle\overrightarrow{\lambda},\nabla u^h\right\rangle dx=\sum_{T,M_i\in T}\int_T\tilde{\alpha}_i^T\left\langle\overrightarrow{\lambda},\nabla u^h\right\rangle dx=\sum_{T,M_i\in T}\tilde{\alpha}_i^T\Phi^T=0 \tag{5}$$

The Residual Distribution discretization is obtained with the obvious choice $\tilde{\alpha}_i^T=\beta_i^T$.

We now turn our attention to the unsteady counterpart of (1), namely

$$\frac{\partial u}{\partial t}+\left\langle\overrightarrow{\lambda},\nabla u\right\rangle=0\text{ in }\Omega\times(0,T). \tag{6}$$

A consistent Residual Distribution discretization is readily obtained through the Petrov-Galerkin approach. If, for example, we choose to use the test function $w_i=\mathcal{N}_i+\alpha_i^T$, we obtain:

$$\sum_{T\in\tau_h}\int_T w_i\frac{\partial u^h}{\partial t}\,dx+\sum_{T\in\tau_h}\int_T w_i\langle\overrightarrow{\lambda},\nabla u^h\rangle\,dx=0. \tag{7}$$

Straightforward algebra leads to the final expression

$$\sum_{T\in\tau_h}\sum_{M_j\in T}m_{ij}^T\frac{d\,u_j}{dt}+\sum_{T,M_i\in T}\Phi_i^T=0 \tag{8}$$

where (m_{ij}^T) is the consistent mass matrix defined by $m_{ij}^T=\int_T w_i\mathcal{N}_j\,dx$:

$$(m_{ij}^T)=\frac{|T|}{3}\begin{bmatrix}\beta_1^T+1/6 & \beta_1^T-1/12 & \beta_1^T-1/12\\ \beta_2^T-1/12 & \beta_2^T+1/6 & \beta_2^T-1/12\\ \beta_3^T-1/12 & \beta_3^T-1/12 & \beta_3^T+1/6\end{bmatrix}. \tag{9}$$

If instead of w_i we use the piecewise constant test function $\tilde{w}_i$, we end up with the expression

$$\sum_{T\in\tau_h}\sum_{M_j\in T}\tilde{m}_{ij}^T\frac{d\,u_j}{dt}+\sum_{T,M_i\in T}\Phi_i^T=0 \tag{10}$$

where $(\tilde{m}_{ij}^T)$ is defined by $\tilde{m}_{ij}^T=\int\limits_T\tilde{w}_i\mathcal{N}_j\,dx$:

$$(\tilde{m}_{ij}^T)=\frac{|T|}{3}\begin{bmatrix}\beta_1^T & \beta_1^T & \beta_1^T\\ \beta_2^T & \beta_2^T & \beta_2^T\\ \beta_3^T & \beta_3^T & \beta_3^T\end{bmatrix}. \tag{11}$$

Remark 2.1. *The first order N-scheme [26] cannot be obtained from a Petrov-Galerkin approach since Φ_i^T/Φ^T are unbounded for vanishing cell residuals.*

Remark 2.2. *Starting from (8) (or equivalently (10)) we can derive a certain number of schemes, extensions of standard Residual Distribution schemes that have the property Φ_i^T/Φ^T bounded (see [20]).*

For steady computations an accurate discretization of the time derivative is not required, so normally one reaches the steady solution through a pseudo-time formulation obtained by lumping the mass matrix, *i.e.* by lumping the elements of each column to the diagonal. This leads to the following inconsistent formulation

$$|C_i|\frac{d\,u_i}{dt}+\sum_{T,M_i\in T}\Phi_i^T=0. \tag{12}$$

An explicit Euler scheme for the time derivative leads to

$$u_i^{n+1}=u_i^n-\frac{\Delta t}{|C_i|}\sum_{T,M_i\in T}\Phi_i^T \tag{13}$$

For steady computations (12) is a good alternative in place of (8) or (10) which require the solution of a system of non linear algebraic equations. With this approximation only first order accuracy can be achieved for unsteady problems even if we use second or third accurate schemes for time derivative. So a consistent formulation is needed to reach high order accuracy. One of the aims of this paper is to show how to construct consistent mass matrices without losing stability properties of the schemes for steady state.

The development of monotone high accurate schemes using (8) has been considered by Ferrante [20] with a flux corrected transport formulation. He has shown that positivity is lost with this formulation (the mass matrix is not guaranteed to be a L-matrix), and to recover monotonicity he used the Flux Corrected Transport to damp the spurious oscillations. This approach works reasonably well, but it is not a natural extension of (13). We lose properties of the Residual Distribution methods like

(i) upwinding;

(ii) linearity preservation;

(iii) compactness of the stencil (due to the FCT limiting).

The aim of this paper is to show how one can recover properties (i), (ii) and (iii).

3 Residual Distribution Schemes for unsteady scalar advection equations

We have shown, in the previous section, that the Residual Distribution scheme (13) is not suitable for computing unsteady problems due to the inconsistent treatment of the mass matrix. Schemes with a consistent mass matrix have been considered by Ferrante, Hubbard, Caraeni, Csik *et al.*, [20, 21, 22, 23], etc. Here we present and illustrate another solution for reaching high order accuracy for unsteady scalar advection, and in the final section, we extend it to the compressible Euler equations.

3.1 Principles

Let us consider equation (6) with constant advection speed. The idea is to see in (6) a steady problem in $\mathbb{R}_\xi \times \mathbb{R}_x \times \mathbb{R}_t$ where ξ is an iteration parameter. We first need to define the cell residual. For steady problems the cell residual over a triangle T is defined as the integral over this element of the operator $\langle \overrightarrow{\lambda}, \nabla \rangle$ with the piecewise linear approximation of u on T. Here we solve the unsteady problem like a steady problem, so we define the cell residual as the integral of the differential operator $\partial_t + \langle \overrightarrow{\lambda}, \nabla \rangle$ with a space-time approximation of u on the prismatic element $T \times [t_n, t_{n+1}]$ (see figure 1). We want to define a space-time approximation of u which allow us to get second order of accuracy. In [17] is shown that a necessary condition for second order of accuracy if that $\Phi^T = \mathcal{O}(\Delta t^3, h^3)$. The most natural choice is

$$u^h(x,t) = \frac{t - t_n}{\Delta t} u^{n+1}(x) + \frac{t_{n+1} - t}{\Delta t} u^n(x) \tag{14}$$

where u^n and u^{n+1} are respectively the piecewise linear approximation of u at time t_n and t_{n+1}. Hence we define the residual Φ^T by

$$\Phi^T = \int_{t_n}^{t_{n+1}} \int_T \frac{\partial u^h}{\partial t} + \left\langle \lambda, \nabla u^h \right\rangle \, dx dt. \tag{15}$$

After calculations, we get

$$\Phi^T = \frac{|T|}{3} \sum_{M_i \in T} (u_i^{n+1} - u_i^n) + \frac{\Delta t}{2} \sum_{M_i \in T} k_i (u_i^{n+1} + u_i^n), \tag{16}$$

with $k_i = \overrightarrow{\lambda} \cdot \overrightarrow{n}_i / 2$, being $\overrightarrow{n}_i$ the vector normal to the edge of T facing node i, scaled by its length. The residual (15)-(16) is the fluctuation computed over the prism $K = T \times [t_n, t_{n+1}]$ (see Figure 1). Our approach is a space-time interpretation of the classical Residual Distribution methods with the linear space-time approximation of the solution (14).

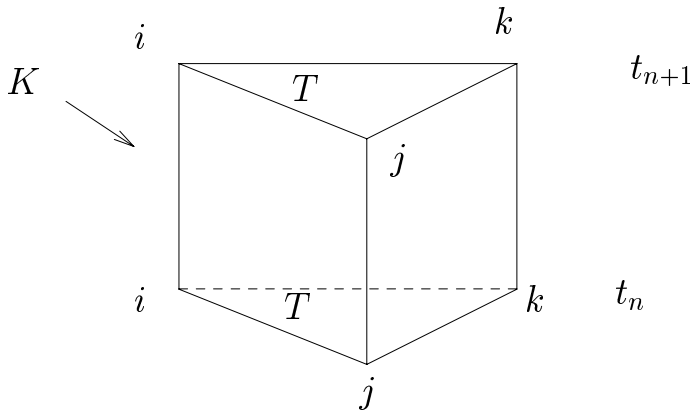

Figure 1: The prism K defined by the triangle T

We need to distribute the fluctuation (16) to the vertices of the prism K. We denote by $\Phi_{i,n}$ and $\Phi_{i,n+1}$ the residuals sent to the nodes (M_i, t_n) and (M_i, t_{n+1}). Upwinding in time, *i.e.* a causality principle, leads us to distribute the time–space residual only to the nodes located at time t_{n+1}, so one has $\Phi_{i,n} = 0$.

The Residual Distribution scheme reads

$$\forall M_i \in \tau_h, \qquad \sum_{T, M_i \in T} \Phi_{i,n+1} = 0, \tag{17}$$

where $\Phi_{i,n+1}$ is the residual sent to node M_i at time t_{n+1}. From now on we replace $\Phi_{i,n+1}$ by Φ_i since there is no possible confusion. The residuals are assumed to fulfill the conservation relation

$$\sum_{M_i \in T} \Phi_i = \Phi^T. \tag{18}$$

where Φ^T is given by (16).

Design principles

(i) **The upwinding property** No fraction of the element residual is sent to nodes for time $t = t_n$. Equation (17) means that all the residual of K is sent to time t_{n+1}.

(ii) **The Linear Preserving condition (LP)** The (LP) property consists in requiring that if the solution is smooth then

$$\Phi_i = \mathcal{O}(h^3, \Delta t^3).$$

In [17] is shown that this is equivalent to ask that $\beta_i = \Phi_i / \Phi^T$ is bounded if Φ^T is computed with enough accuracy. In particular, second order of accuracy is obtained if $\Phi^T = \mathcal{O}(h^3, \Delta t^3)$.

(iii) **No spurious oscillations in the solution**

3.2 Extension of classical schemes

In this section we present a space-time N scheme and LDA scheme that reduce to the standard N and LDA scheme for steady state applications (see [17, 27] for the definition of the schemes). These space-time schemes will allow us to construct non-linear space-time blended and limited schemes.

3.2.1 The LDA scheme

This scheme directly follows from the consistent formulations (8) and (10) with Crank-Nicholson discretization for the time derivative, using the standard LDA-scheme. Consider first expression (8) with the standard LDA-scheme,

$$\sum_{T,M_i\in T}\sum_{M_j\in T} m_{ij}^T \frac{d\,u_j}{dt} + \sum_{T,M_i\in T} \beta_i^{\mathrm{LDA}} \Phi^T(u^h) = 0$$

where $u^h = \sum_j u_j(t)\mathcal{N}_j$, $\beta_i^{\mathrm{LDA}} = -k_i^+ N$ and N is defined by

$$N = \sum_{M_j\in T} k_j^- \,.$$

If we consider a Crank-Nicholson discretization of time derivative we get

$$\begin{aligned}
&\sum_{T,M_i\in T}\sum_{M_j\in T} m_{ij}^T (u_j^{n+1} - u_j^n) + \frac{\Delta t}{2} \sum_{T,M_i\in T} (-k_i^+ N)\left(\Phi^T(u^{n+1}) + \Phi^T(u^n)\right) = 0 \\
&\sum_{T,M_i\in T}\sum_{M_j\in T} m_{ij}^T (u_j^{n+1} - u_j^n) + \frac{\Delta t}{2} \sum_{T,M_i\in T} (-k_i^+ N)\left(\sum_j k_j (u_j^{n+1} + u_j^n)\right) = 0
\end{aligned} \tag{19}$$

After lengthy calculations, expression (19) can be written as

$$\sum_{T,M_i\in T} \Phi_i^{LDA} = 0,$$

with Φ_i^{LDA} defined by

$$\begin{aligned}
\Phi_i^{LDA} =& \frac{|T|}{3}(-k_i^+ N + \frac{1}{6})(u_i^{n+1} - u_i^n) + \\
& \frac{|T|}{3}(-k_i^+ N - \frac{1}{12}) \sum_{M_j\neq M_i} (u_j^{n+1} - u_j^n) - \frac{\Delta t}{2} k_i^+ N \sum_{M_j\in T} k_j (u_j^{n+1} + u_j^n)
\end{aligned} \tag{20}$$

We can rewrite the LDA-scheme as $A\,U^{n+1} = B\,U^n$. The matrices A and B have no apparent properties.

Remark 3.1. *We recover the LDA scheme of Ferrante [20].*

Consider now the formulation (10) with the standard LDA scheme:

$$\sum_{T,M_i\in T}\sum_{M_j\in T} \tilde{m}_{ij}^T \frac{d\,u_j}{dt} + \sum_{T,M_i\in T} (-k_i^+ N)\Phi^T(u^h) = 0$$

After applying a Crank-Nicholson discretization of time derivative we obtain

$$\sum_{T,M_i\in T}\sum_{M_j\in T} \tilde{m}_{ij}^T (u_j^{n+1} - u_j^n) + \frac{\Delta t}{2} \sum_{T,M_i\in T} (-k_i^+ N)\left(\sum_j k_j (u_j^{n+1} + u_j^n)\right) = 0 \tag{21}$$

Also last expression can be recast as

$$\sum_{T,M_i\in T} \Phi_i^{LDA} = 0,$$

with

$$\Phi_i^{LDA} = -k_i^+ N \sum_{M_j \in T} \frac{|T|}{3}(u_j^{n+1} - u_j^n) + (-k_i^+ N)\frac{\Delta t}{2}\left(\sum_j k_j (u_j^{n+1} + u_j^n)\right) = \beta_i^{\mathrm{LDA}} \Phi^T \quad (22)$$

As before we can write the LDA-scheme as $A\,U^{n+1} = B\,U^n$. The matrices A and B have no apparent properties.

Remark 3.2. *We recover the LDA scheme of Caraeni combined with Crank-Nicholson time-integration [22].*

3.2.2 The N scheme

We set

$$\Phi_i^N = \frac{|T|}{3}(u_i^{n+1} - u_i^n) + \frac{\Delta t}{2} k_i^+ (u_i^{n+1} - \widetilde{u}^{n+1}) + \frac{\Delta t}{2} k_i^+ (u_i^n - \widetilde{u}^n).$$

where $\widetilde{u}^n$ and $\widetilde{u}^{n+1}$ are computed to have the conservation relation (18). One gets easily

$$\widetilde{u}^n = N \sum_{M_j \in T} k_j^- u_j^n, \qquad \widetilde{u}^{n+1} = N \sum_{M_j \in T} k_j^- u_j^{n+1}$$

The residual for node i becomes

$$\Phi_i^N = \frac{|T|}{3}(u_i^{n+1} - u_i^n) + \frac{\Delta t}{2} \sum_{M_j \in T} \left[k_i^+ N k_j^- (u_i^{n+1} - u_j^{n+1}) + k_i^+ N k_j^- (u_i^n - u_j^n)\right]. \quad (23)$$

The schemes reads, for all $M_i \in \tau_h$

$$\sum_{T, M_i \in T} \left[\frac{|T|}{3}(u_i^{n+1} - u_i^n) + \frac{\Delta t}{2} \sum_{M_j \in T} \left[k_i^+ N k_j^- (u_i^{n+1} - u_j^{n+1}) + k_i^+ N k_j^- (u_i^n - u_j^n)\right]\right] = 0. \quad (24)$$

Remark 3.3.

1. *For steady computations, we recover the standard N-scheme.*
2. *One of the reasons for splitting space and time like equation (23) is that the conservation relation is met and positivity can be shown (see below). Another constraint comes from the fact the scheme (24) is implicit in time : the linear system has to be solvable. This last point was a motivation for the present splitting.*

The scheme (24) is an implicit scheme, which can be written as $A\,U^{n+1} = B\,U^n$ where U^{n+1} and U^n are respectively the vectors of unknowns at time t_{n+1} and t_n. The entries of the matrices A and B are given by

$$A_{ii} = \sum_{T, M_i \in T} \left(\frac{|T|}{3} + \frac{\Delta t}{2} k_i^+\right) \quad , \quad A_{ij} = \sum_{T, (M_i, M_j) \in T} -\frac{\Delta t}{2} k_i^+ N k_j^- \quad (25)$$

$$B_{ii} = \sum_{T, M_i \in T} \left(\frac{|T|}{3} - \frac{\Delta t}{2} k_i^+\right) \quad , \quad B_{ij} = \sum_{T, (M_i, M_j) \in T} \frac{\Delta t}{2} k_i^+ N k_j^- \quad (26)$$

We have the following lemma :

Lemma 3.4. *The matrix A is non singular and is a L-matrix i.e. $A_{ii} > 0$ $\forall i$ and $A_{ij} \leq 0$ for $j \neq i$.*

Proof. One has $A_{ii} > 0$, and $A_{ij} \leq 0$ since $N < 0 \rightarrow k_i^+ N k_j^- \geq 0$, hence A is a L-matrix.

To prove that A is non-singular we show that A is a diagonally strictly dominant matrix i.e.

$$\forall i \quad |A_{ii}| > \sum_{j \neq i} |A_{ij}|$$

We have

$$\begin{aligned}
|A_{ii}| - \sum_{M_j \neq M_i} |A_{ij}| &= \sum_{T, M_i \in T} (\frac{|T|}{3} + \frac{\Delta t}{2} k_i^+) - \sum_{M_j \neq M_i} \sum_{T, (M_i, M_j) \in T} \frac{\Delta t}{2} k_i^+ N k_j^- \\
&= \sum_{T, M_i \in T} (\frac{|T|}{3} + \frac{\Delta t}{2} k_i^+) - \sum_{T, M_i \in T} \sum_{M_j \neq M_i} \frac{\Delta t}{2} k_i^+ N k_j^- \\
&= \sum_{T, M_i \in T} (\frac{|T|}{3} + \frac{\Delta t}{2} k_i^+) - \sum_{T, M_i \in T} \frac{\Delta t}{2} k_i^+ \\
&= \sum_{T, M_i \in T} \frac{|T|}{3} \\
&= |C_i| > 0
\end{aligned}$$

This shows that A is diagonally strictly dominant. This achieves the proof. □

We remark that $B_{ij} \geq 0$ for $j \neq i$, and under the condition $\Delta t \leq \frac{2}{3} \frac{|T|}{k_i^+}$ one has $B_{ii} \geq 0$. The monotonicity property of the scheme is described in the following :

Proposition 3.5. *The extension of the N-scheme defined by (24) is monotone under the CFL like condition*

$$\Delta t \leq \frac{2}{3} \min_{T, M_i \in T} \frac{|T|}{k_i^+}. \tag{27}$$

Remark 3.6.

1. *This result states that the scheme is monotonicity preserving, at least under a CFL like condition. This is a statement of stability in the L^∞ norm. This is not a statement on the L^2 stability, in other words, we are not saying that this implicit scheme is only stable under the condition (27). To anticipate a bit the results of this paper, we show in appendix A in a more complex case for which the scalar one is a very particular example, that this scheme is* unconditionally *stable in L^2.*

2. *The condition (27) seems to be a severe limit on the allowed time step but computations with CFL great than one have shown that monotonicity is preserved. A close look at the proof indicates that this condition is certainly not optimal. In section (5), we show two different approaches allowing to avoid or improve this severe constraint.*

Proof. The scheme can be written as $A\,U^{n+1} = B\,U^n$ with A a non singular L-matrix, and B a matrix with positive elements. It is shown in [28] that if A is a regular L-matrix the following assertions are equivalent

(i) A^{-1} is positive,

(ii) there exists a diagonal positive matrix D such that $D^{-1}AD$ is diagonally strictly dominant.

We apply this results with $D = Id$ so it implies that A^{-1} is positive. B has positive elements, thus the matrix $A^{-1}B$ is positive.

• ***Step 1 :*** Suppose there exists $a \in \mathbb{R}$ such that $u_i^n \geq a$ for all $M_i \in \tau_h$. One wants to show $u_i^{n+1} \geq a$ for all $M_i \in \tau_h$.

One has

$$\sum_{M_i \in T} \left(\frac{|T|}{3}(u_i^{n+1} - u_i^n) + \frac{\Delta t}{2} \sum_{M_j \neq M_i} k_i^+ N k_j^- (u_i^{n+1} - u_j^{n+1} + u_i^n - u_j^n) \right) = 0$$

hence

$$\begin{array}{c} \sum_{M_i \in T} \left(\frac{|T|}{3} u_i^{n+1} + \frac{\Delta t}{2} \sum_{M_j \neq M_i} k_i^+ N k_j^- (u_i^{n+1} - u_j^{n+1}) \right) = \\ \sum_{M_i \in T} \left(\frac{|T|}{3} u_i^{n} - \frac{\Delta t}{2} \sum_{M_j \neq M_i} k_i^+ N k_j^- (u_i^{n} - u_j^{n}) \right) = \\ \sum_{M_i \in T} \left((\frac{|T|}{3} - \frac{\Delta t}{2} k_i^+) u_i^n + \frac{\Delta t}{2} \sum_{M_j \neq M_i} k_i^+ N k_j^- u_j^n \right) \geq \\ \sum_{M_i \in T} \left((\frac{|T|}{3} - \frac{\Delta t}{2} k_i^+) a + \frac{\Delta t}{2} \sum_{M_j \neq M_i} k_i^+ N k_j^- a \right) \geq \sum_{M_i \in T} \frac{|T|}{3} a \end{array} \tag{28}$$

because the matrix B is positive. The inequalities (28) imply that

$$\sum_{M_i \in T} \left(\frac{|T|}{3}(u_i^{n+1} - a) + \frac{\Delta t}{2} \sum_{j \neq i} k_i^+ N k_j^- ((u_i^{n+1} - a) - (u_j^{n+1} - a)) \right) \geq 0,$$

which can be rewritten as

$$A(u^{n+1} - a) \geq 0.$$

The matrix A^{-1} is positive so one has $u^{n+1} - a \geq 0$, *ie* $u_i^{n+1} \geq a$ for all $M_i \in \tau_h$.

• ***Step 2 :*** Suppose that there exists $a \in \mathbb{R}$ such that $u_i^n \leq a$ for all $M_i \in \tau_h$. One wants to show $u_i^{n+1} \leq a$ for all $M_i \in \tau_h$. We do the same thing as before. This achieves the proof. □

3.2.3 The PSI scheme

The extension of the PSI scheme is obtained in a straightforward way following the approach of [17]. The scheme is a result of a combination of the first order monotone N-scheme (24) and the second order non-monotone LDA-scheme (20)

$$\Phi_i^{PSI} = l\Phi_i^N + (1 - l)\Phi_i^{LDA}. \tag{29}$$

where $l = \max(\varphi(r_1), \varphi(r_2), \varphi(r_3))$ with

$$r_i = \frac{\Phi_i^{LDA}}{\Phi_i^N}, \qquad \varphi(x) = \begin{cases} \dfrac{x}{1-x} \text{ if } x < 0 \\ 0 \text{ else} \end{cases}$$

We have experimentally noticed that the blending parameter, proposed for steady state by Deconinck and van der Weide, defined by

$$l = \frac{|\Phi^T|}{\sum\limits_{M_j \in T} |\Phi_j^N|} \tag{30}$$

works very well, even though it does not satisfy the positivity requirements (we have found numerical counter-examples).

Being the PSI scheme non-linear, we need to solve a system of non linear equations even in the case of the scalar linear problem (6). This is done by Newton's method. One can write the PSI scheme as $F(U^{n+1}) = 0$,

$$\begin{aligned} F: \quad & \mathbb{R}^{ns} \to \mathbb{R}^{ns} \\ & U \mapsto (F_i(U))_{i=1,\dots,ns} \end{aligned}$$

where $F_i(U) = \sum\limits_{T, M_i \in T} \Phi_i^{PSI}$ and ns is th number of nodes in τ_h. The kth step of Newton's method is

$$U^{k+1} = U^k - \widetilde{J}(U^k) F(U^k),$$

where $\widetilde{J}(U^k) = \partial F / \partial U$ evaluated at point U^k.

3.2.4 The N-Modified scheme

The N-Modified scheme is described in [24]. We set

$$\phi_i^{NM} = \Phi_i^N + \Psi_i = \beta_i^{NM} \Phi^T, \tag{31}$$

Ψ_i is computed to get second order accuracy and positivity *exactly* or, in other words, Ψ_i is computed such that β_i^{NM} is always bounded. In [24] several ways of defining β_i^{NM} (or equivalently Ψ_i) are discussed. One of the most effective ways of doing it is the following:

$$\beta_i^{NM} = \frac{\left(\beta_i^N\right)^+}{\sum\limits_{M_j \in T} \left(\beta_j^N\right)^+} \tag{32}$$

with $\beta_i^N = \Phi_i^N / \Phi^T$. Definition (32) combined with (31) leads to

$$\phi_i^{NM} = \alpha \Phi_i^N \quad , \quad \alpha = \frac{\beta_i^{NM}}{\beta_i^N} \geq 0 \tag{33}$$

which implies the positivity of the scheme. Moreover β_i^{NM} is bounded, which implies that the modified scheme is linearity preserving.

Remark 3.7. *The space-time N modified scheme can be written using the Petrov-Galerkin formulation (10).*

As in the case of the PSI scheme, the N modified scheme is non-linear, the non-linearity being in the definition of β_i^{NM}. Hence it leads always to a non-linear system of equations. The non linear equations are solved using a Newton algorithm.

3.3 Numerical Results

3.3.1 The rotating cosine hill

The rotating cosine hill is a classical test-case for numerical schemes of the two-dimensional linear unsteady advection equation. The test consists in the transport of a cosine shape by a circular advection field centered at the origin

$$\frac{\partial u}{\partial t} + \left\langle \overrightarrow{\lambda}, \nabla u \right\rangle = 0 \quad \text{in } [-1,1] \times [-1,1], \tag{34}$$

where $\lambda = (y, -x)^T$. The initial solution is $(1 + \cos(4\pi\sqrt{(x+0.5)^2 + y^2}))/2$ if $r = \sqrt{(x+0.5)^2 + y^2} \leq \frac{1}{8}$ and 0 elsewhere . The computation was made on an unstructured grid of 8079 nodes and 15836 elements. The time step was taken to satisfy the condition (27) :

$$\Delta t = \frac{2}{3}\, CFL \min_i \frac{|T|}{k_i^+}, \tag{35}$$

with $CFL = 0.9$. The solution is set to zero at the inflow boundaries at each time step. The results, using the schemes described in the previous section and the MUSCL scheme (with *minmod* limiter and Runge-Kutta integration in time) after one revolution are compared in Figure 2. We provide the cross–section at $y = 0$ on Figure 3. The results obtained with scheme (22) (referred as LDA1 scheme in table 1) are given in figure 4. In the PSI and blended schemes we used (20).

On the figures we see that the N-scheme is clearly the most diffusive (see also Table 1), stream-wise and crosswise diffusion being considerable. The LDA schemes keep the height of the peak much better but the monotonicity is not preserved. The PSI and N-modified schemes give similar results but the N-modified scheme is the less diffusive with a peak value of 0.802. These results are much better than those obtained by the MUSCL scheme.

Scheme	min	max
N	0	0.217
MUSCL	0	0.313
LDA	-0.03	0.983
LDA1	-0.08	1.03
PSI	0	0.756
N-modified	0	0.802

Table 1: Min and Max solution values for the rotating cosine hill test case.

3.3.2 The rotating cylinder

This test case differs from the previous only for the initial profile

$$u(x,y) = \begin{cases} 1 & \text{for } r < 0.25, \\ 0 & \text{else} \end{cases} \tag{36}$$

where $r = \sqrt{(x+0.5)^2 + y^2}$, which is not continuous, contrary to the previous case. The computation was made on the same grid with a CFL of 0.9, the results after one revolution being displayed in figures 5, 6 and 7.

As in the case of the rotation of the cosine hill, the PSI scheme and N-modified scheme give very close results. These results are better than the ones obtained with the MUSCL scheme. The LDA schemes exhibit spurious oscillations, as expected. In particular, Caraeni's version of the LDA scheme (see [22] and Remark 3.2) are very oscillatory. This is not a linear stability problem, since the results on the cosine advection are excellent (see figure 4).

In both cases, the limited N scheme and the blended–PSI behave the same. However, the modified N scheme CPU cost is about half that of the blended scheme, because one has no need to evaluate the LDA scheme.

3.4 Conclusions for the scalar problems

We have considered two different techniques for increasing the accuracy of unsteady problems, the PSI–blending and the N–modified schemes. The results are roughly speaking similar, with a slight advantage for the N–modified scheme, in term of accuracy and efficiency. On unstructured meshes, both schemes yield considerably better results than classical MUSCL schemes.

The extension to systems of equations is possible for both techniques. In particular for the PSI–blending technique one can follow [17]. This has been done elsewhere and we do not report the results here. This technique works quite well but in some cases, for example the interaction of a vortex and a shock (see §4.3.4) or the ramp problem (see §4.3.3), the results are disappointing : monotonicity is not very well preserved across the shocks.

For these reasons we have abandoned the PSI–blending technique, and we do not consider it anymore in the paper.

We remark that in [29] the author has developped a different class of space-time schemes for unsteady scalar advection which also work on prismatic elements. In the reference the author presents results obtained with these schemes on the rotation of the cosine hill and of the cylinder on regular meshes finer than the one used here. These results are considerably more dissipative than the ones obtained with the approach proposed here, although they are still better than the MUSCL results (which again favours the residual distribution approach). Moreover, although the author presents an extension of his schemes to the non-linear inviscid Burger's equation, the extension to the Euler equations is not clear at all.

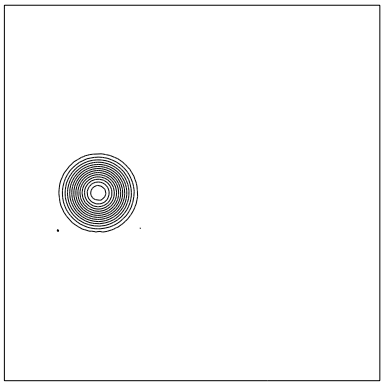

Exact solution

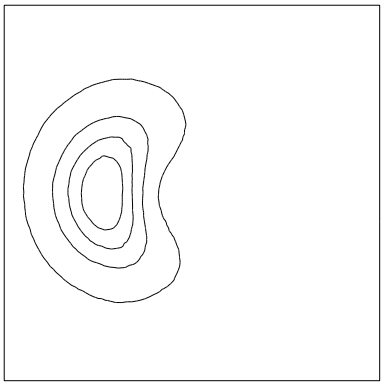

N

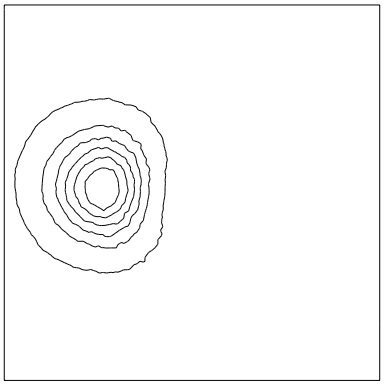

MUSCL

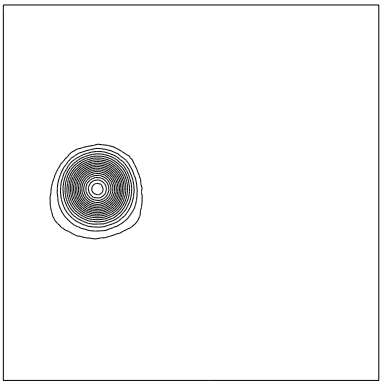

LDA

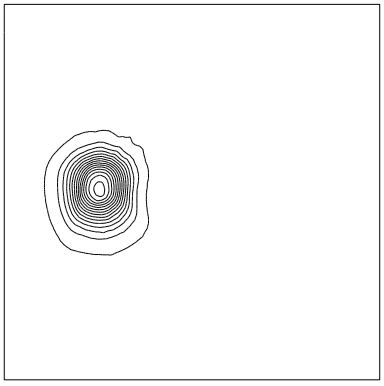

PSI

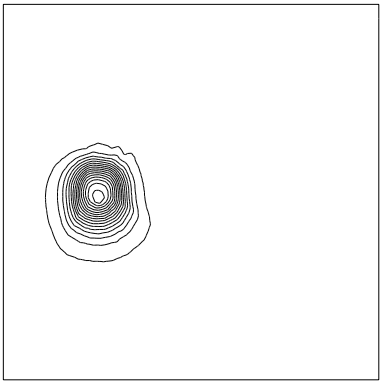

N-modified

Figure 2: Solutions for the rotating cosine hill after one revolution

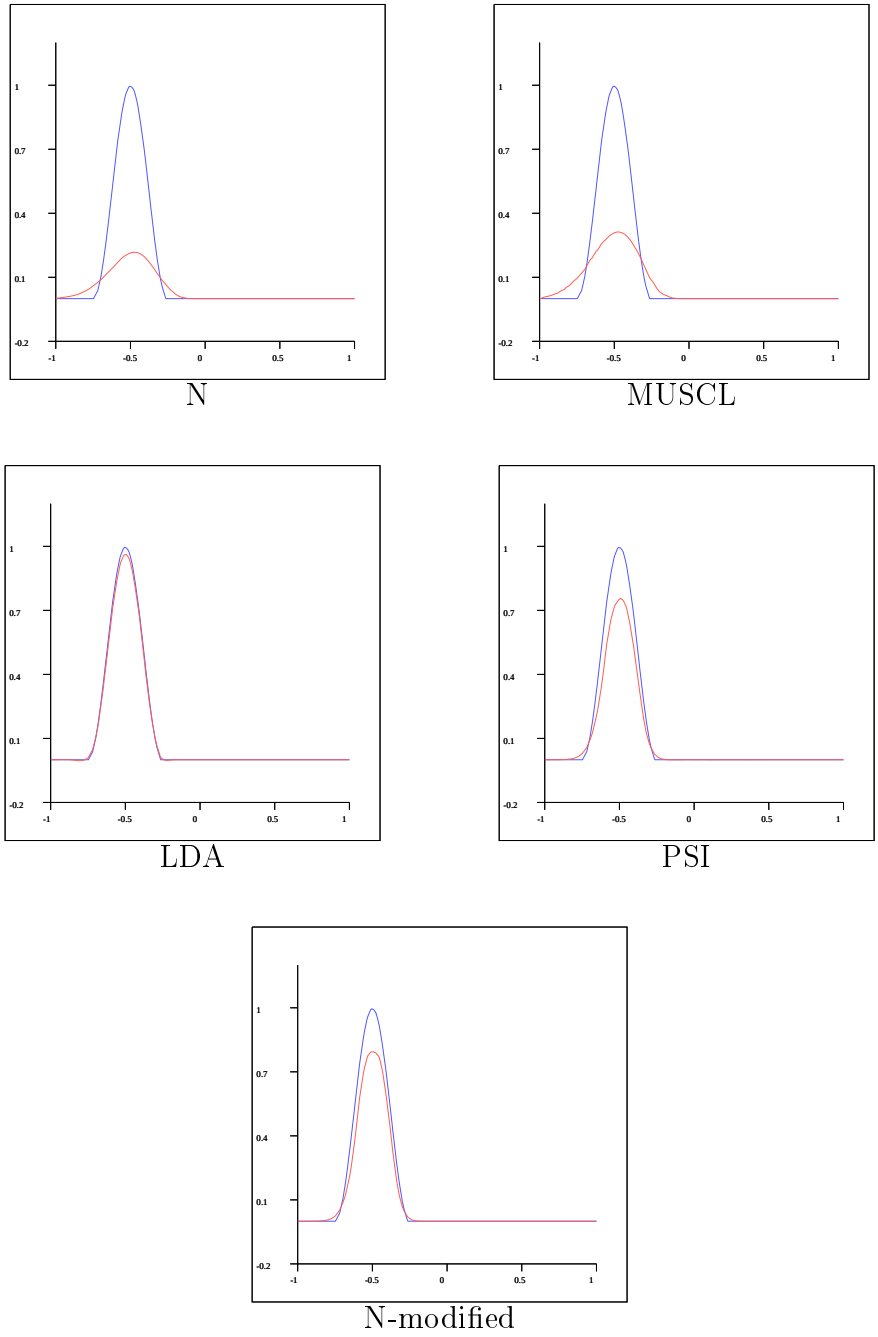

Figure 3: Sections at y=0 of the solutions for the rotating cosine

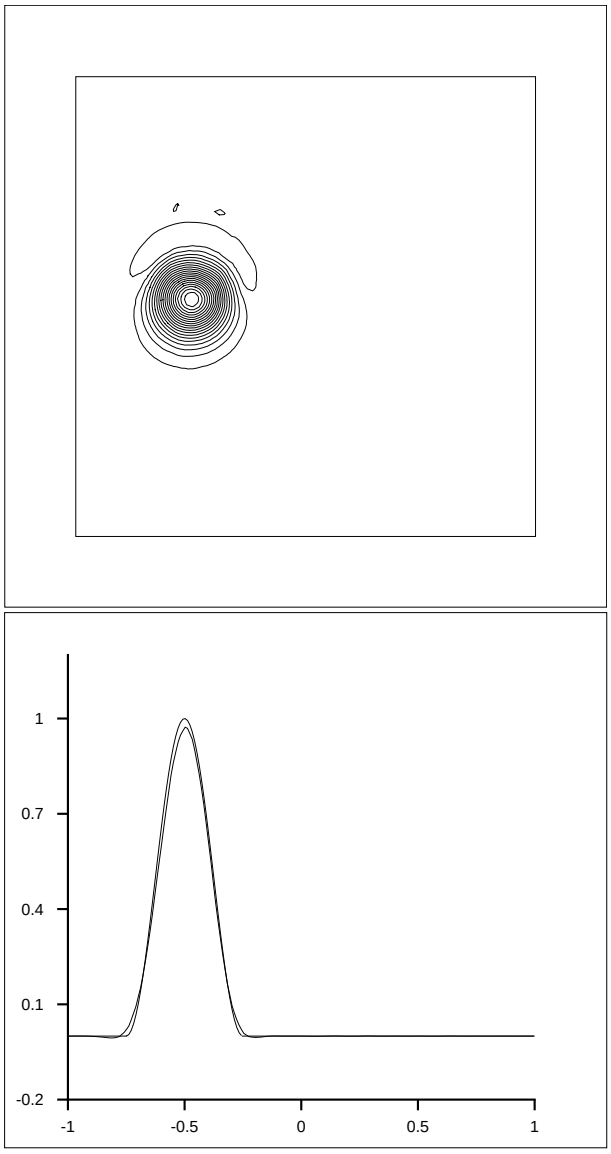

Figure 4: Contour and cross–section for Caraeni's LDA scheme on the cosine problem.

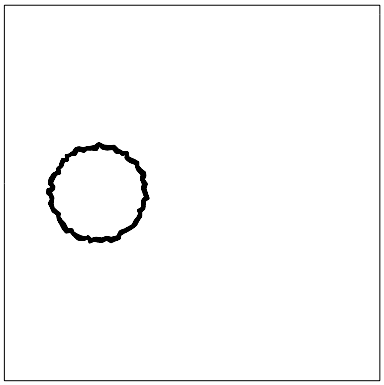

Exact solution

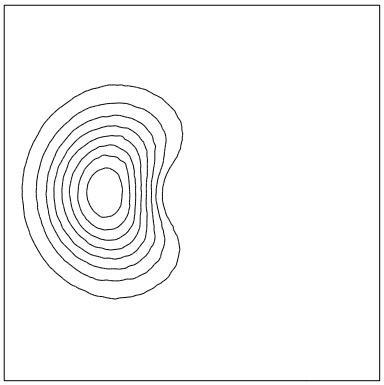

N

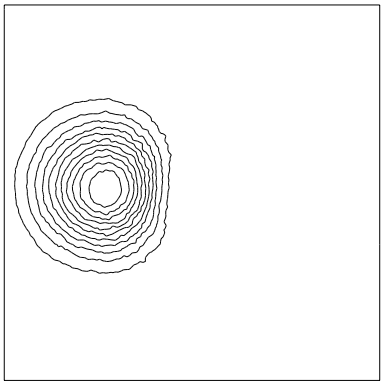

MUSCL

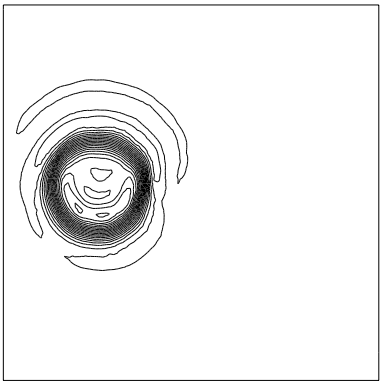

LDA

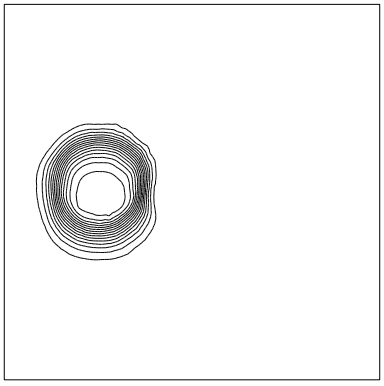

PSI

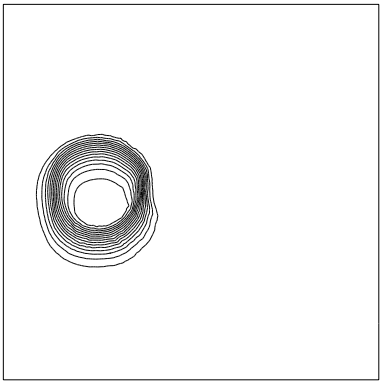

N-modified

Figure 5: Solutions for the rotating cylinder after one revolution.

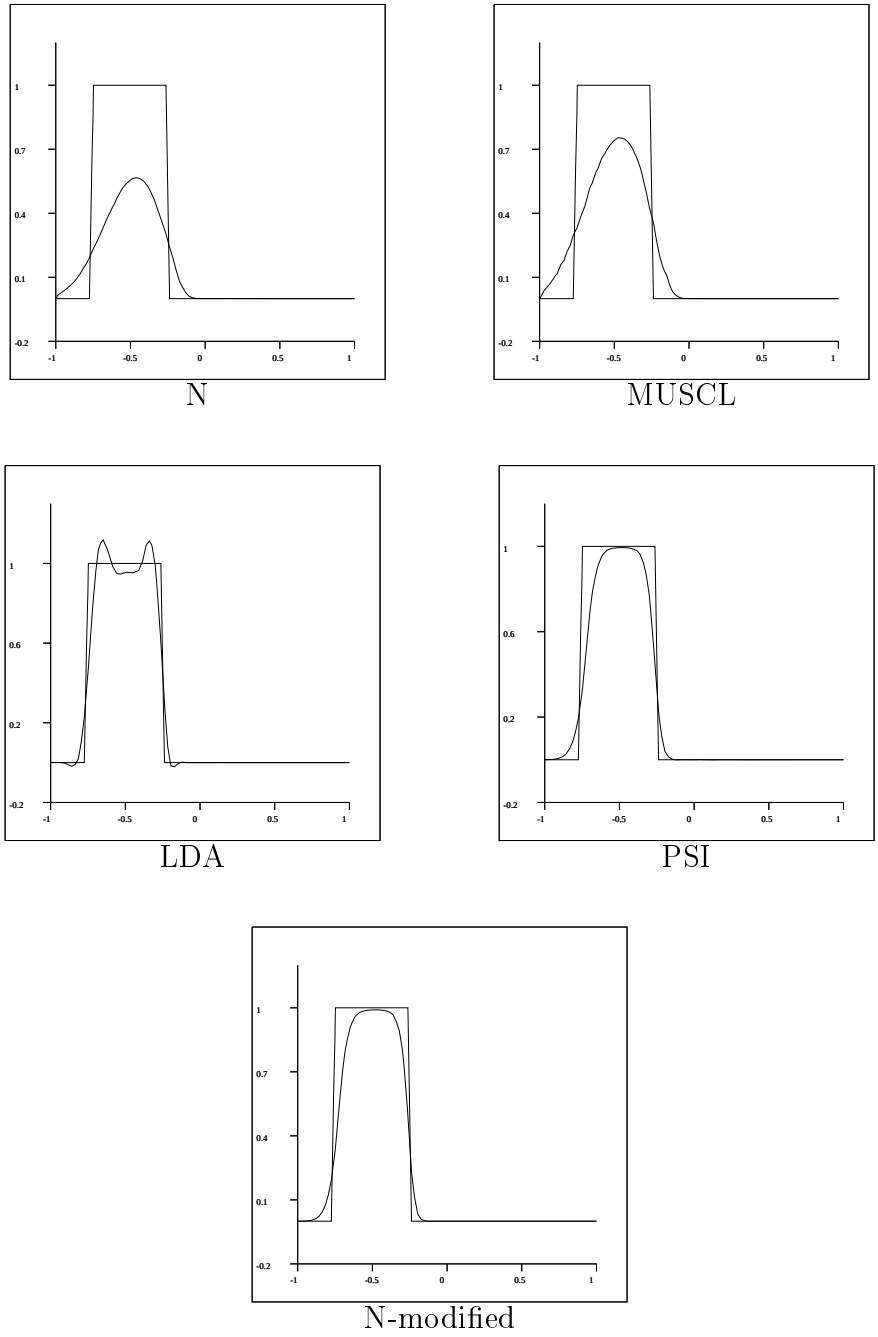

Figure 6: Sections at y=0 of the solutions for the rotating cylinder

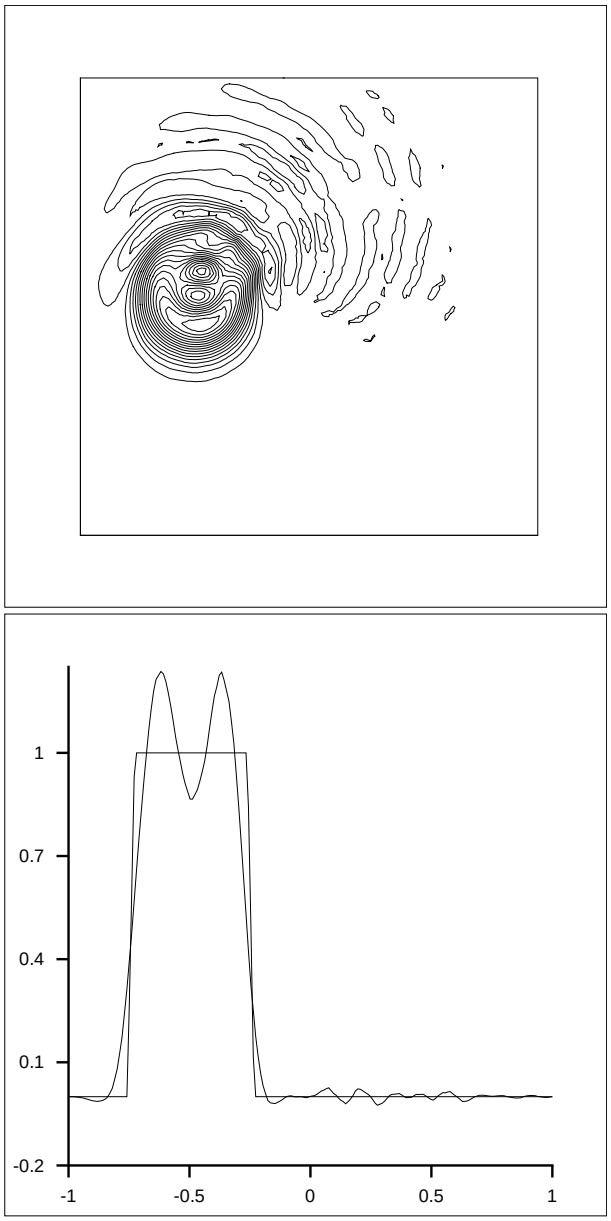

Figure 7: Contour and cross-section for Caraeni's LDA scheme on the cylinder problem. Min=−0.35, Max=1.41.

4 Residual Distribution Schemes for the unsteady Euler equations

Consider the system of the Euler equations

$$\frac{\partial W}{\partial t} + \text{ div } \mathbf{F}(W) = 0,$$

where W and $\mathbf{F} = (F, G)$ are given by

$$\begin{array}{l} W = (\rho, \rho u, \rho v, E)^T, \\ F(W) = (\rho u, \rho u^2 + p, \rho uv, u(E+p))^T, \\ G(W) = (\rho v, \rho uv, \rho v^2 + p, v(E+p))^T \end{array} \tag{37}$$

where ρ, u and v are the gas density and velocity components, E is the total energy and p the pressure. The system is closed by the perfect gas equation of state.

The construction of the Residual Distribution schemes, described in the previous section, is based on the quasi-linear form of the convection equations (as for steady schemes) and a space-time approximation of the unknowns. So extension to the unsteady Euler equations needs to use :

(i) a second order approximation of W and $\mathbf{F}$ in order to get second order accuracy;

(ii) a conservative linearization.

4.1 The cell residual

The cell residual over a prism $T \times [t_n, t_{n+1}]$ is given by

$$\Phi^T = \int_{t_n}^{t_{n+1}} \int_T \left(\frac{\partial W^h}{\partial t} + \text{ div } \mathbf{F}^h \right) dxdt,$$

where W^h and $\mathbf{F}^h$ are respectively the space-time approximation of the solution and the fluxes. This approximation is obtained using Roe's parameter vector Z:

$$Z = (\sqrt{\rho}, \sqrt{\rho}u, \sqrt{\rho}v, \sqrt{\rho}H)^T \tag{38}$$

where H is defined by the relation $H = (E+p)/\rho$. We set

$$\begin{array}{rcl} W^h & = & \dfrac{t - t_n}{\Delta t} W^{n+1} + \dfrac{t_{n+1} - t}{\Delta t} W^n, \\ \mathbf{F}^h & = & \dfrac{t - t_n}{\Delta t} \mathbf{F}^{n+1} + \dfrac{t_{n+1} - t}{\Delta t} \mathbf{F}^n, \end{array}$$

where $W^s = W(Z^s)$ and $\mathbf{F}^s = \mathbf{F}(Z^s)$ and Z^s being the piecewise linear approximation of Z at time s (t_n or t_{n+1}). One has $\Phi^T = I_1 + I_2$, with

$$I_1 = \int_{t_n}^{t_{n+1}} \int_T \frac{\partial W^h}{\partial t} \, dxdt, \qquad I_2 = \int_{t_n}^{t_{n+1}} \int_T \text{ div } \mathbf{F}^h dxdt.$$

We recall that for the Euler equations we can express W and $\mathbf{F}$ as

$$W = \frac{1}{2} D(Z) Z \qquad \mathbf{F} = \frac{1}{2}(R_1(Z)Z, R_2(Z)Z) = \frac{1}{2}\mathcal{R}(Z)Z$$

where the matrices $D(Z)$, $R_1(Z)$ and $R_2(Z)$ are linear in Z (see [24]).
For I_1 we have then

$$I_1 = \int_{t_n}^{t_{n+1}} \int_T \frac{\partial W}{\partial t}\, dxdt = \int_T \frac{D(Z^{n+1})Z^{n+1} - D(Z^n)Z^n}{2}\, dx.$$

Moreover, since $D(Z)Z$ is quadratic in Z and $D(Z)$ is linear in Z, we have

$$\begin{aligned}
\int_T D(Z)Z\, dx &= \frac{|T|}{3}\left(D(\frac{Z_1+Z_2}{2})\frac{Z_1+Z_2}{2} + D(\frac{Z_1+Z_3}{2})\frac{Z_1+Z_3}{2} + D(\frac{Z_2+Z_3}{2})\frac{Z_2+Z_3}{2}\right) \\
&= \frac{|T|}{12}\sum_{M_i\in T} D(Z_i)Z_i + \frac{|T|}{4}\sum_{M_i\in T} D(\overline{Z})Z_i \\
&= \frac{|T|}{6}\sum_{M_i\in T} W_i + \frac{|T|}{4}\sum_{M_i\in T} \widetilde{W}_i,
\end{aligned}$$

with $\widetilde{W}_i = D(\overline{Z})Z_i$ and $\overline{Z}$ is the Roe average state $\overline{Z} = (Z_1+Z_2+Z_3)/3$ [30].
Finally I_1 becomes

$$I_1 = \frac{|T|}{4}\sum_{M_j\in T}\left[(\frac{1}{3}W_j^{n+1} + \frac{1}{2}\widetilde{W}_j^{n+1}) - (\frac{1}{3}W_j^n + \frac{1}{2}\widetilde{W}_j^n)\right].$$

Now we compute I_2

$$\begin{aligned}
I_2 &= \int_{t_n}^{t_{n+1}} \int_T \text{div } \mathbf{F}\; dxdt = \frac{\Delta t}{2}\int_T \text{div } \mathbf{F}^{n+1} + \text{ div } \mathbf{F}^n\; dx \\
&= \frac{\Delta t}{2}\int_T \mathcal{R}(Z^{n+1})\, dx\nabla Z^{n+1} + \frac{\Delta t}{2}\int_T \mathcal{R}(Z^n)\, dx\nabla Z^n \\
&= \frac{\Delta t}{2}\sum_{M_j\in T} \frac{\mathcal{R}(\overline{Z}^{n+1}).n_j^T}{2} Z_j^{n+1} + \frac{\mathcal{R}(\overline{Z}^n).n_j^T}{2} Z_j^n.
\end{aligned}$$

Setting $K_j^{n+1} = \frac{1}{2}\left\langle \mathcal{R}(\overline{Z}^{n+1})D^{-1}(\overline{Z}^{n+1}), n_j^T\right\rangle$ and $K_j^n = \frac{1}{2}\left\langle \mathcal{R}(\overline{Z}^n)D^{-1}(\overline{Z}^n), n_j^T\right\rangle$, the cell residual can be finally expressed as

$$\begin{aligned}
\Phi^T = &\frac{|T|}{4}\sum_{M_j\in T}\left[(\frac{1}{3}W_j^{n+1} + \frac{1}{2}\widetilde{W}_j^{n+1}) - (\frac{1}{3}W_j^n + \frac{1}{2}\widetilde{W}_j^n)\right] \\
&+ \frac{\Delta t}{2}\sum_{M_j\in T}\left(K_j^{n+1}\,\widetilde{W}_j^{n+1} + K_j^n\,\widetilde{W}_j^n\right),
\end{aligned} \tag{39}$$

where $\widetilde{W}_j^n = D(\overline{Z}^n)Z_j^n$ and $\widetilde{W}_j^{n+1} = D(\overline{Z}^{n+1})Z_j^{n+1}$.

The final expression is similar to (16), but a difficulty appears with the presence of terms K_j^{n+1} which are computed at time t_{n+1} (due to the non-linearity of the Euler equations). Therefore system Residual Distribution schemes for unsteady computations are intrinsically implicit in time. This is solved thanks to a Newton method.

4.2 System residual distribution schemes

In this section we give the generalization of the unsteady scalar schemes described in section 3.2.

4.2.1 The system LDA scheme

We will present here only the extension to the Euler equation of scheme (20). The system version of scheme (22) can be obtained in a similar way. In particular, we set

$$\begin{aligned}\Phi_i^{LDA} =&(-(K_i^+N)^{n+1}+\frac{1}{6}\mathrm{Id})\Phi_i^t+\\ &(-(K_i^+N)^{n+1}-\frac{1}{12}\mathrm{Id})\sum_{M_j\neq M_i}\Phi_j^t-(K_i^+N)^{n+1}\Phi^s\end{aligned}$$

where we have set

$$\Phi_j^t=\frac{|T|}{4}\left[(\frac{1}{3}W_j^{n+1}+\frac{1}{2}\widetilde{W}_j^{n+1})-(\frac{1}{3}W_j^n+\frac{1}{2}\widetilde{W}_j^n)\right]\ ,$$

$$\Phi^s=\frac{\Delta t}{2}\sum_{j\in T}K_j^{n+1}\,\widetilde{W}_j^{n+1}+K_j^n\,\widetilde{W}_j^n$$

and

$$N^n=(\sum_{M_j\in T}K_j^{n-})^{-1}\ \ ,\ \ N^{n+1}=(\sum_{M_j\in T}K_j^{n+1^-})^{-1}\,.$$

Remark 4.1. *The matrices $N^nK_j^n$ and $N^{n+1}K_j^{n+1}$ always exist (see [17]), so the system LDA-scheme is well defined.*

4.2.2 The system N-scheme

For a scalar advection equation one has

$$\phi_i^N=\frac{|T|}{3}(u_i^{n+1}-u_i^n)+\frac{\Delta t}{2}k_i^+(u_i^{n+1}-\widetilde{u}^{n+1})+\frac{\Delta t}{2}k_i^+(u_i^n-\widetilde{u}^n),\tag{40}$$

where $\widetilde{u}^n$ and $\widetilde{u}^{n+1}$ are computed to have the conservation relation (18). For the Euler equations we set

$$\begin{aligned}\phi_i^N=&\frac{|T|}{4}\left[(\frac{1}{3}W_i^{n+1}+\frac{1}{2}\widetilde{W}_i^{n+1})-(\frac{1}{3}W_i^n+\frac{1}{2}\widetilde{W}_i^n)\right]\\ &+\frac{\Delta t}{2}K_i^{n+1^+}(\widetilde{W}_i^{n+1}-W_{n+1}^*)+\frac{\Delta t}{2}K_i^{n+}(\widetilde{W}_i^n-W_n^*).\end{aligned}\tag{41}$$

If W_{n+1}^* and W_n^* are computed to make the scheme conservative, namely

$$W_{n+1}^*=N^{n+1}\sum_{M_j\in T}K_j^{n+1^-}\widetilde{W}_j^{n+1},\quad W_n^*=N^n\sum_{M_j\in T}K_j^{n^-}\widetilde{W}_j^n\tag{42}$$

Remark 4.1 also applies to the N scheme.

In the appendix A, we show that this system is unconditionally energy–stable.

4.2.3 The system N-modified scheme

The idea is similar to the one developed in [24]. We present here a summary of these results, and we refer to the above reference for a detailed presentation.

For sake of simplicity, let us explain our procedure on the linearized $d \times d$ system

$$\frac{\partial W}{\partial t} + A\frac{\partial W}{\partial x} + B\frac{\partial W}{\partial y} = 0$$

with A and B symmetric matrices. Since for any (α, β) the matrix $\alpha A + \beta B$ is symmetric, there exists a complete set of eigenvectors $\{r_j\}_{j=1,d}$. Following [24], we introduce the simple waves

$$U_\sigma(x,t) = \big(t - t_0\big)\ \big(\alpha x + \beta y\big) r_\sigma$$

where r_σ is an eigenvector in $\{r_j\}_{j=1,d}$ and λ_σ is the associated eigenvalue. We note that any function

$$W(x,t) = \frac{t - t_n}{\Delta t} W^{n+1}(x) + \frac{t_{n+1} - t}{\Delta t} W^n(x)$$

where W^n and W^{n+1} are linear in x, is a sum of $3 \times d \times 2$ simple waves plus possibly a constant. This number of waves comes from the fact that a triangle has 3 vertices, so there are 3 basis functions, any vector $W \times \mathcal{N}_j(x)$ can be decomposed into the sum of d orthogonal vectors, and we have to do so at times t_n and t_{n+1}. More precisely, W^n (resp. W^{n+1}) can be written as

$$\begin{aligned} W^n(x) &= \sum_{j=1}^{3} W_j^n \mathcal{N}_j(x) \\ &= \text{constant} + \frac{1}{2|T|} \sum_{j=1}^{3} W_j^n \langle \overrightarrow{n}_j, x \rangle \end{aligned}$$

where $\overrightarrow{n}_j$ is the inward normal opposite to the jth vertex of triangle T. If we take $\overrightarrow{n}_j = (\alpha_j, \beta_j)^T$ and decompose W_j^n on an eigenvector basis of $\alpha_j A + \beta_j B$ denoted by $\{r_k^j\}_{k=1,d}$ we recognize that

$$\big(t - t_n\big) \langle W_j^n, r_k^j \rangle \langle \overrightarrow{n}_k, x \rangle r_k^j$$

is precisely a simple wave.

In summary, any function piecewise linear in time and space can be decomposed into the sum of $3 \times d \times 2$ simple waves

$$\begin{aligned} U_\sigma(x,t) &= \left(\frac{t - t_n}{\Delta t} \big(\alpha^{n+1} x + \beta^{n+1} y\big) + \frac{t_{n+1} - t}{\Delta t} \big(\alpha^n x + \beta^n y\big) \right) r_\sigma \\ &= \left(\frac{t - t_n}{\Delta t} \varphi^{n+1}(x) + \frac{t_{n+1} - t}{\Delta t} \varphi^n(x) \right) r_\sigma. \end{aligned}$$

Then, following once more [24], it is possible to show that the N scheme (40) is monotone on any simple wave. This means that the residual Φ_i^N sent to the node i can be written, for a simple wave, as a linear combination of terms like

$$\sum_{j=1,3} \big(c_{ij}^k\big)^{n+1} \Big(\varphi_j^{n+1} - \varphi_i^{n+1} \Big) r_j^k \quad \text{and} \quad \sum_{j=1,3} \big(c_{ij}^k\big)^{n} \Big(\varphi_j^{n} - \varphi_i^{n} \Big) r_j^k \tag{43}$$

where φ_j is the value of φ at the jth vertex of T, $c_{ij}^k \geq 0$ and $k = 1, d$.

Using the above analysis, we introduce the modified N scheme as follows: we take a direction (α, β), consider the eigenvectors of $\alpha A + \beta B$ and write the residual of the N scheme as

$$\Phi_i^N = \sum_{k=1}^{d} \varphi_i^k r_k, \qquad \varphi_i^k = \langle \Phi_i^N, r_k \rangle$$

We then modify the scalar residual $\{\varphi_i^k\}_{i=1,3}$ exactly as in section 3.2.4. We note that

$$\sum_{i=1}^{3} \varphi_i^k = \langle \Phi, r_k \rangle.$$

Following [24], and using relations (43), it is possible to show that the system modified N scheme is stable.

In the case of a symmetrizable system, we proceed along the same lines. The only modification is that the scalar products between a state variable W or a residual Φ_i^N with an eigenvector r_k are replaced by the inner product between W (resp. Φ_i^N) and the *left* eigenvector ℓ_k associated to the right eigenvector r_k. In fact, it is known that if A_0 is the symmetrization matrix, $A_0 r_k = \ell_k$, so if we make the change of variable $V = A_0 W$, we come back to the symmetric case.

In the previous description, the choice of the direction (α, β) is arbitrary. Different choices will produce different results, and different schemes. However, all our numerical experiments for steady and unsteady problems lead to the conclusion that the quality of the results is independent of the direction (α, β). By quality, we mean the non oscillatory properties of the schemes, and the mesh resolution of the different features of the solution. In all the numerical experiments we present in this paper for fluid problems, we have chosen the vector (α, β) to be the local flow velocity vector, for symmetry reasons mainly.

4.3 Numerical Results

In this section we present results on some classical test cases obtained with the schemes presented in the previous section. For Euler computations, we replace condition (27) by

$$\Delta t \leq \frac{2}{3} \min_{T, M_i \in T} \frac{|T|}{\lambda_i^+}, \tag{44}$$

where λ_i^+ is the largest positive eigenvalue of K_i^n.

4.3.1 Two-dimensional Sod's Riemann Problem

The initial data are chosen in order to represent a two-dimensional version of Sod's shock tube problem in the domain $[-1, 1] \times [-1, 1]$:

$$\left\{ \begin{array}{rcl} \rho & = & 0.1 \text{ if } x \times y < 0, \ 1 \text{ otherwise} \\ p & = & 0.1 \text{ if } x \times y < 0, \ 1 \text{ otherwise} \end{array} \right. \tag{45}$$

The velocity (u, v) is initially set to zero everywhere. The solution is computed at time t=0.2 on a structured triangulation where $\Delta x = \Delta y = 0.01$. The CFL number in (44) has been set to 0.9.

The isolines of the density and pressure are shown in Figures 8 and 9 for the N-scheme and the N-modified scheme.

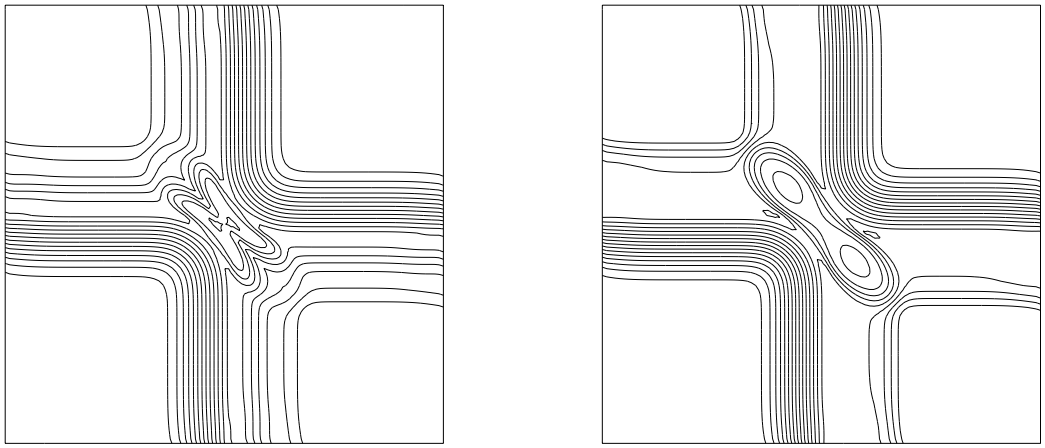

Figure 8: 2D Sod problem computed by the N-scheme at time t=0.2, density (left) and pressure (right).

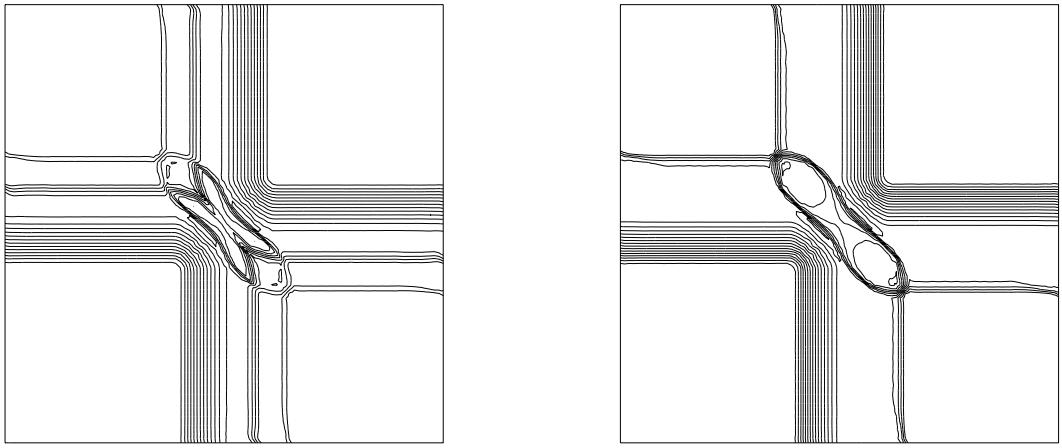

Figure 9: 2D Sod problem computed by the N-modified scheme at time t=0.2, density (left) and pressure (right).

4.3.2 A Mach 3 Wind Tunnel with a Forward Facing Step

This test case has been extensively studied by Woodward and Collela [31], and it is widely present in the literature. The setup of the problem is the following : a right-going Mach 3 uniform flow enters a wind tunnel of 1 unit width and 3 units long. The tunnel contains a forward facing step of height 0.2 units located 0.6 units from the left end of the tunnel. The problem is initialized by a uniform, right going Mach 3 flow. Reflective boundary conditions are applied along the walls of the tunnel, and inflow and outflow boundary conditions are applied at the entrance and the exit of the tunnel. The corner of the step is a singularity and it is well known that if no special treatment is adopted in this point an excessive entropy production is observed which alters the quality of the second reflected shock. This is not physical because at the corner we have an isentropic expansion wave, so no entropy should be created. However, unlike in [31], we do not modify our scheme near the corner, since we are only interested in the stability properties of the schemes.

We have run the simulation on an unstructured mesh containing 10,868 nodes and 21,281 triangles. The mesh is refined near the corner. A portion of the mesh is shown in Figure 10. The simulation was done at CFL$= 0.9$.

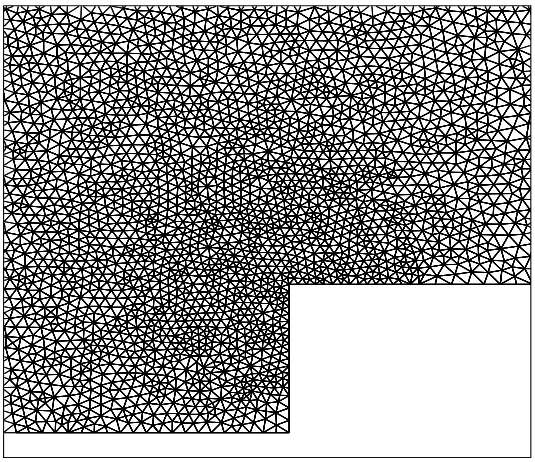

Figure 10: Part of the unstructured grid for the Mach 3 problem.

The results obtained with the N scheme and N modified scheme at time 0.4 are given in figures 11,12 and 13. We see that the quality of the slip line coming out of the triple point is noticeable, as well as the resolution of the shocks, in particular at the exit section of the tunnel. The maximum shock width is no larger than two cells. Between the first order and the second order results, the quality of the fan (at the corner) has dramatically been improved : the reflected shock is now correctly set, the weak compression shock after the fan appears, and interacts with the first reflected shock. We also see the slip line coming out of the interaction between the reflected shock and the weak compression shock.

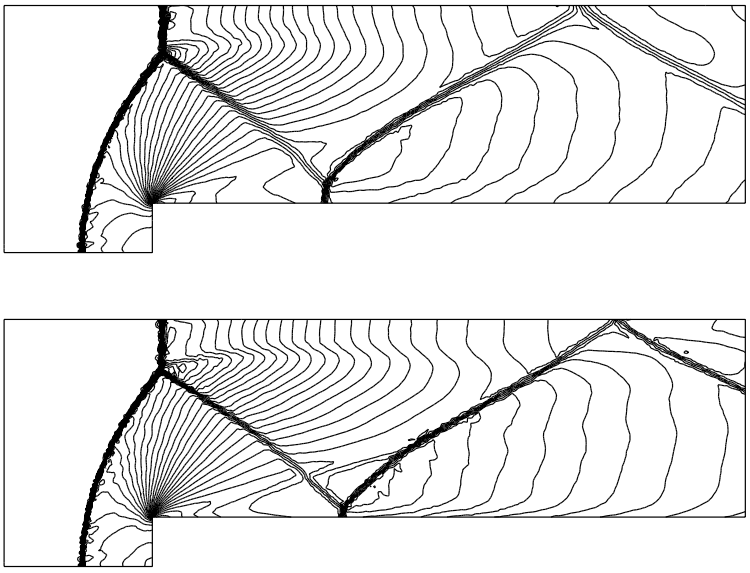

Figure 11: Forward-facing step problem. Density iso-lines: 30 equally spaced contour lines from 0.09 to 6.23. Top : N scheme. Bottom : N-modified scheme.

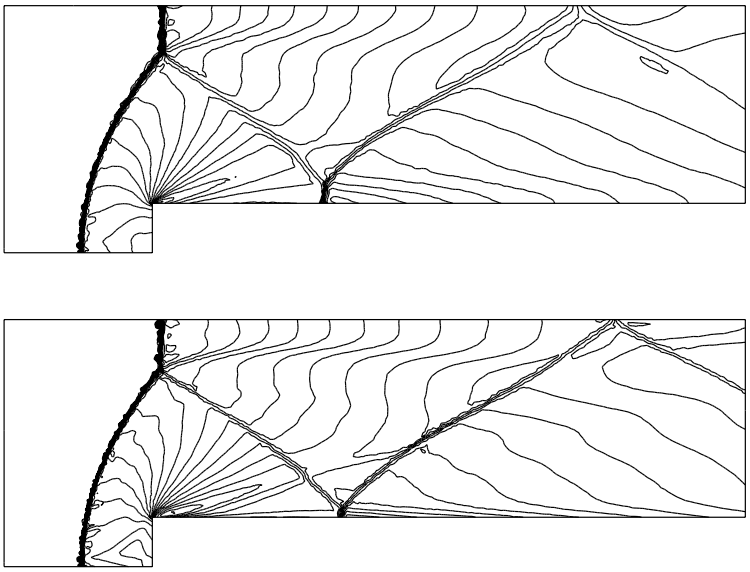

Figure 12: Forward-facing step problem. Mach number iso-lines: 25 equally spaced contour lines from 0.02 to 3.82. Top : N scheme. Bottom : N-modified scheme.

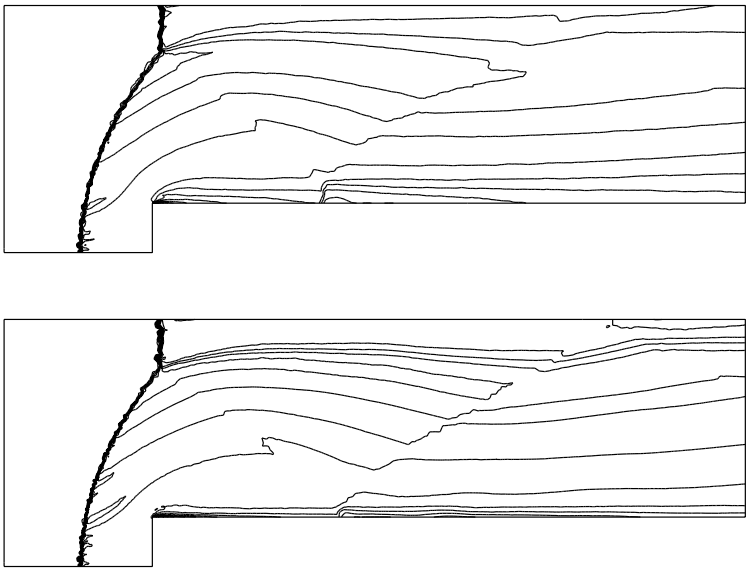

Figure 13: Forward-facing step problem. Entropy production near the step corner : 17 equally spaced contour lines from 0.63 to 1.5., Top : N scheme. Bottom :N-modified scheme.

4.3.3 Reflection of a Shock on a Wedge

This problem was studied by Quirk [32]. A planar shock initially enters from the left in a quiescent fluid and is reflected from a 45 degrees ramp. The shock Mach number, defined with respect to the flow values in the quiescent fluid, is $M_s = 5.5$. In the quiescent gas ahead of the shock the density is set to 1.4 and the pressure to 1. Reflective boundary conditions are applied along the ramp and the bottom and the upper of the problem domain. Inflow and outflow boundary conditions are applied at the entrance and the exit

of the domain. For this combination of shock Mach number and ramp angle, a double Mach reflection is expected. The interest of this test case is that , according to [33], the angle $\theta = 45^o$ and $M_s = 5.5$ is nearly at the transition between a double Mach reflection and a regular reflection. If the scheme would be too diffusive, we would get a regular reflection instead of a double Mach reflection. Hence this is a good test of accuracy.

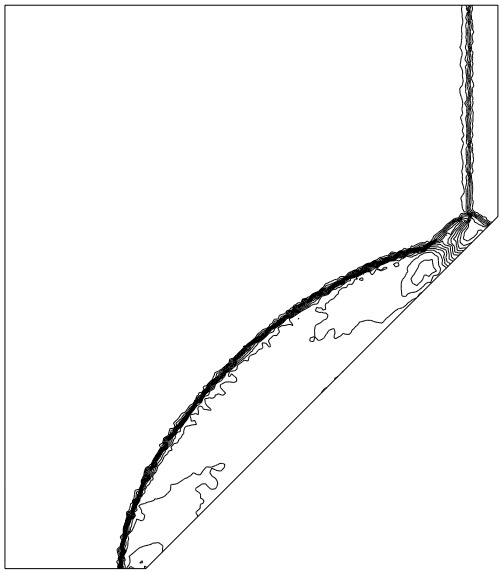

Figure 14: Reflection of a planar shock from a ramp. Density 20 contour lines from 1.18 to 20.12.

The density for the N-modified scheme is displayed in Figure 14. The CFL number has been set to 0.9. The resolution of the different structures is quite clean, despite of the poor resolution of the mesh.

4.3.4 Shock-Vortex Interaction Problem

This test case describes the interaction between a stationary shock and a vortex. It was first presented by Pao and Salas [34], and was studied by Meadows *et al.* [35] with a TVD scheme and by Jiang and Shu [36]. The computational domain is taken to be $[0, 2] \times [0, 1]$. A stationary Mach 1.1 shock is set at $x = 0.5$ and normal to the x-axis. Its left state is $(\rho, u, v, p) = (1, \sqrt{\gamma}, 0, 1)$. A small vortex is superposed to the flow left of the shock and centered at $(x_c, y_c) = (0.5, 0.25)$. The vortex is described as a perturbation to the velocity (u, v), temperature $T = \frac{p}{\rho}$ and entropy $S = \ln \frac{p}{\rho^\gamma}$ of the mean flow denoted by tilde values:

$$\tilde{u} = \epsilon\tau e^{\alpha(1-\tau^2)} \sin\theta \quad (46)$$

$$\tilde{v} = -\epsilon\tau e^{\alpha(1-\tau^2)} \cos\theta \quad (47)$$

$$\tilde{T} = -\frac{(\gamma-1)\epsilon^2 e^{2\alpha(1-\tau^2)}}{4\alpha\gamma} \quad (48)$$

$$\tilde{S} = 0 \quad (49)$$

where $\tau = \frac{r}{r_c}$ and $r = \sqrt{(x-x_c)^2 + (y-y_c)^2}$. Here ϵ indicates the strength of the vortex, α controls the decay rate of the vortex, and r_c is the critical radius for which the vortex

has the maximum strength. We choose the same values as in [36], *i.e.* $\epsilon = 0.3$, $r_c = 0.05$ and $\alpha = 0.204$. The above defined vortex is a steady solution to the 2D Euler equations. The upper and lower boundary are set to be reflective. We use a uniform grid of 251×100, a zoom of which is shown on Figure 15. Also for this test we took $CFL = 0.9$.

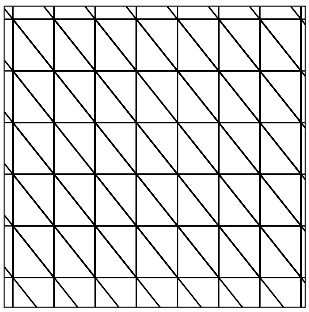

Figure 15: Zoom of the mesh for the vortex simulation.

The pressure isolines for the N-modified scheme at three different times are displayed in Figure 16.

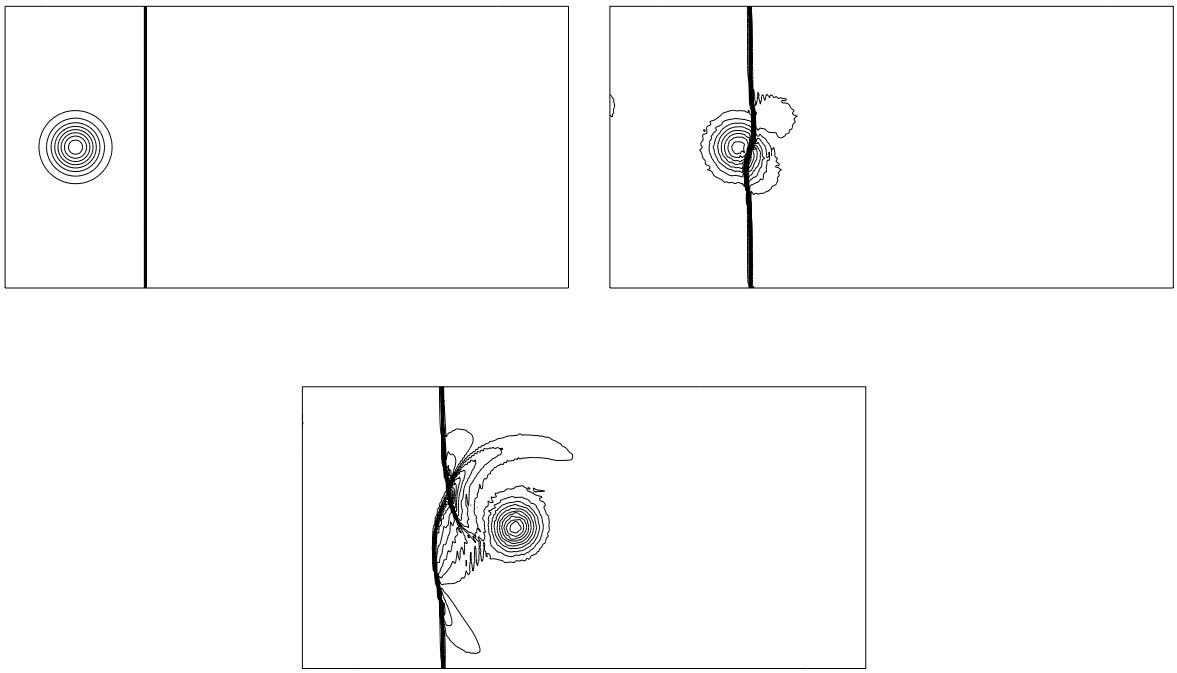

Figure 16: Shock vortex interaction. Pressure. N-modified scheme. 30 contours lines from 0.84 to 1.4. Top left: t=0; Top right: t=0.2, Bottom: t=0.4.

5 Toward unconditionally monotone and LP schemes

The objective of this section is the construction of unconditionally stable monotone LP space-time schemes. In particular, we will illustrate two different techniques which allow us to build non-linear schemes for which monotonicity is not constrained by (27). We start by building an unconditionally stable linear first order N scheme which utilizes the two-layers approach introduced in [16]. We will analyze the monotonicity of the scheme and then present results obtained on the Euler equations with its modified variant.

We then present a different approach to construct a non-linear LP scheme which is not constrained by (27). We first present an unconditionally stable N scheme which does not respect the conservation constraint (18). We then borrow from [25] the idea of constructing a modified scheme which respects (18) starting by the non-conservative N scheme. We analyze the monotonicity properties of the scheme and present scalar and Euler simulations showing the stability and accuracy of the modified scheme.

5.1 A two-layers unconditionally monotone LP scheme

Let us consider the scalar advection equation

$$\frac{\partial u}{\partial t} + \left\langle \overrightarrow{\lambda}, \nabla u \right\rangle = 0 \quad \text{in } \Omega \times [0,T]. \tag{50}$$

The N-scheme reads

$$\Phi_i^N = \frac{|T|}{3}(u_i^{n+1} - u_i^n) + \frac{\Delta t}{2} \sum_{M_j \in T} k_i^+ N k_j^- (u_i^{n+1} - u_j^{n+1} + u_i^n - u_j^n). \tag{51}$$

By construction, the N scheme is upwind in the prismatic element K : no contribution is sent to the past node located at time t_n (upwinding in time). In [16] the authors have introduced a different class of space-time schemes which work on P1 space-time elements (triangles in 1 space dimension and tetrahedra in two space dimensions). The authors show that by straightforward application of the standard steady-state residual distribution schemes, upwinding in time can be obtained, provided that the space-time mesh is properly constructed and satisfies a constraint on its time width very similar to (27). To overcome this limitation, the authors have introduced a second layer of space-time elements in which dependence of the past solution from the future one is allowed. By solving for two time levels at once they have obtained an unconstrained scheme which they have "experimentally" shown to have good monotonicity properties.

Here we exploit the same idea but on a greatly simplified (and less expensive) framework : we use prismatic elements. In particular, we consider three levels of nodes with temporal coordinates t_n, $t_{n+\alpha}$ and t_{n+1}, $\alpha \in [0,1]$. This delimits two layers of space-time prismatic elements. Considering a triangle T, we denote by K_1 and K_2 the prisms delimited by T contained in the first and the second layer, with time thickness $\Delta t_1 = t_{n+\alpha} - t_n$ and $\Delta t_2 = t_{n+1} - t_{n+\alpha}$ (see Figure 17).

5.1.1 Description of an unconditionally monotone scheme

Starting from the space-time N-scheme (23), which was made on a single layer of elements, we reformulate it on two layers of elements to allow us an unconditionally stable time marching procedure while maintaining monotonicity both in space and time.

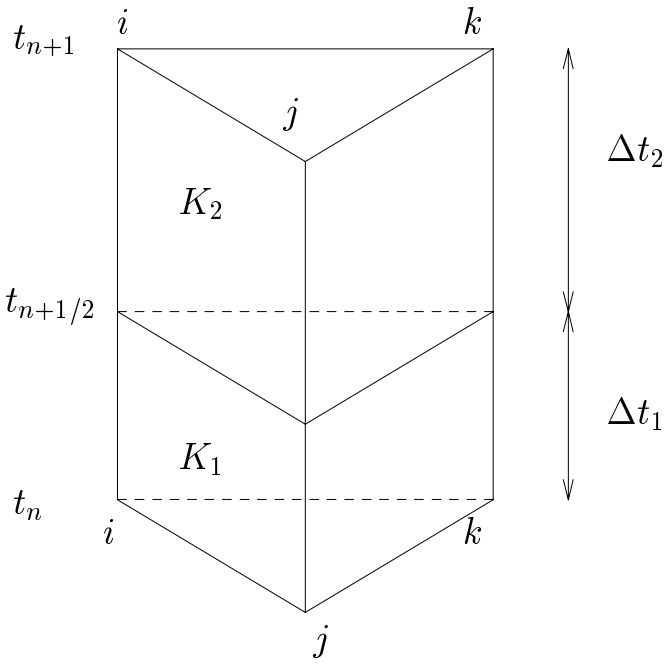

Figure 17: Space-time grid for the two-layers unconditionally monotone and stable scheme.

We denote by $\Phi_{i,n}$, $\Phi_{i,n+\alpha}$ and $\Phi_{i,n+1}$ the residual sent to nodes (M_i, t_n), $(M_i, t_{n+\alpha})$ and (M_i, t_{n+1}). In the first layer, the past does not depend on the future, that is to say $\Phi_{i,n}^{K_1} = 0$. We set

$$\Phi_{i,n+\alpha}^{K_1} = \frac{|T|}{3}(u_i^{n+\alpha} - u_i^n) + \frac{\Delta t_1}{2} \sum_{M_j \in T} k_i^+ N k_j^- (u_i^{n+\alpha} - u_j^{n+\alpha} + u_i^n - u_j^n) \tag{52}$$

In the second layer we do not impose the upwind property, ie $\Phi_{i,n+\alpha}^{K_2} \neq 0$. We set

$$\Phi_{i,n+\alpha}^{K_2} = \frac{\Delta t_2}{2} \sum_{M_j \in T} k_i^+ N k_j^- (u_i^{n+\alpha} - u_j^{n+\alpha}) \tag{53}$$

$$\Phi_{i,n+1}^{K_2} = \frac{|T|}{3}(u_i^{n+1} - u_i^{n+\alpha}) + \frac{\Delta t_2}{2} \sum_{M_j \in T} k_i^+ N k_j^- (u_i^{n+1} - u_j^{n+1}) \tag{54}$$

Finally the scheme reads

$$\sum_{K,(i,n+\alpha)\in K} \Phi_{i,n+\alpha}^K = 0 \quad \text{and} \sum_{K,(i,n+1)\in K} \Phi_{i,n+1}^K = 0. \tag{55}$$

We explain now in detail the contribution to each node:

- For the node$(M_i, t_{n+\alpha})$ one has

$$\begin{aligned} \Phi_{i,n+\alpha}^{K_1} + \Phi_{i,n+\alpha}^{K_2} =& \frac{|T|}{3}(u_i^{n+\alpha} - u_i^n) + \frac{\Delta t_1}{2} \sum_{M_j \in T} k_i^+ N k_j^- (u_i^{n+\alpha} - u_j^{n+\alpha} + u_i^n - u_j^n) \\ &+ \frac{\Delta t_2}{2} \sum_{M_j \in T} k_i^+ N k_j^- (u_i^{n+\alpha} - u_j^{n+\alpha}) \end{aligned} \tag{56}$$

$$\Phi^{K_1}_{i,n+\alpha} + \Phi^{K_2}_{i,n+\alpha} = \frac{|T|}{3}(u_i^{n+\alpha} - u_i^n) + \frac{\Delta t_1}{2}(1 + \frac{\Delta t_2}{\Delta t_1}) \sum_{M_j \in T} k_i^+ N k_j^- (u_i^{n+\alpha} - u_j^{n+\alpha}) + \frac{\Delta t_1}{2} \sum_{M_j \in T} k_i^+ N k_j^- (u_i^n - u_j^n) \tag{57}$$

Assembling the contributions of all the elements one obtains $Au^{n+\alpha} = Bu^n$ with

$$A_{ii} = \sum_{T, M_i \in T} (\frac{|T|}{3} + \frac{\Delta t_1}{2}(1 + \frac{\Delta t_2}{\Delta t_1}) k_i^+) \quad , \quad A_{ij} = \sum_{T, (M_i, M_j) \in T} -\frac{\Delta t_1}{2}(1 + \frac{\Delta t_2}{\Delta t_1}) k_i^+ N k_j^- \tag{58}$$

$$B_{ii} = \sum_{T, M_i \in T} (\frac{|T|}{3} - \frac{\Delta t_1}{2} k_i^+) \quad , \quad B_{ij} = \sum_{T, (M_i, M_j) \in T} \frac{\Delta t_1}{2} k_i^+ N k_j^- . \tag{59}$$

The matrix B has positive entries if Δt_1 satisfies condition (27). The inverse of A always exists and has positive entries for all choices of the time steps Δt_1, Δt_2.

• For the node (M_i, t_{n+1}), assembling contributions of all elements gives $Au^{n+1} = Bu^{n+\alpha}$ with

$$A_{ii} = \sum_{T, M_i \in T} (\frac{|T|}{3} + \frac{\Delta t_2}{2} k_i^+) \quad , \quad A_{ij} = \sum_{T, (M_i, M_j) \in T} -\frac{\Delta t_2}{2} k_i^+ N k_j^- . \tag{60}$$

$$B_{ii} = \sum_{T, M_i \in T} \frac{|T|}{3} k_i^+ \quad , \quad B_{ij} = 0. \tag{61}$$

The matrices B and A^{-1} always have positive elements for all choices of time step Δt_2.

The time-step for the first layer (Δt_1) is limited by a CFL-like condition, as we have seen in the previous section for the space-time N-scheme. However, since we do not impose an upwinding condition in time for the second layer, an arbitrary time-step Δt_2 can be chosen. Then the global time-step $\Delta t = \Delta t_1 + \Delta t_2$ is not constrained by any CFL like condition. We have constructed a scheme with unconditionally stable implicit time stepping which maintains full monotonicity.

The extension to the Euler equations is obtained easily combining (52), (53) and (41).

5.1.2 An unconditionally monotone and LP scheme

Limiting the contributions in the prisms K_1 and K_2, we obtain a monotone and LP scheme. In particular, from the residuals $\Phi^{K_1}_{i,n+\alpha}$, $\Phi^{K_2}_{i,n+\alpha}$ and $\Phi^{K_2}_{i,n+1}$ we construct modified residuals $\Phi^{K_1 *}_{i,n+\alpha}$, $\Phi^{K_2 *}_{i,n+\alpha}$ and $\Phi^{K_2 *}_{i,n+1}$ as described in section 3.2.4:

• In the prism K_1, we construct $\Phi^{K_1 *}_{i,n+\alpha}$ such that

$$\sum_{M_j \in T} \Phi^{K_1 *}_{j,n+\alpha} = \Phi^{K_1} \tag{62}$$

$$\Phi^{K_1 *}_{i,n+\alpha} = \mathcal{O}(h^3, \Delta t^3) \tag{63}$$

• In the prism K_2, we construct $\Phi^{K_2 *}_{i,n+\alpha}$ and $\Phi^{K_2 *}_{i,n+1}$ such that

$$\sum_{M_j \in T} \left[\Phi^{K_2 *}_{j,n+\alpha} + \Phi^{K_2 *}_{j,n+1} \right] = \Phi^{K_2} \tag{64}$$

$$\Phi^{K_2 *}_{i,n+\alpha} = \mathcal{O}(h^3) + \mathcal{O}(\Delta t^3) \tag{65}$$

$$\Phi^{K_2 *}_{i,n+1} = \mathcal{O}(h^3) + \mathcal{O}(\Delta t^3) \tag{66}$$

Then the solution is advanced from time t_n to time t_{n+1} by the following procedure

1. From t_n to $t_{n+\alpha}$. Compute the state at time $t_{n+\alpha}$ by solving

$$\sum_{T, M_i \in T} \left(\Phi^{K_1^*}_{i,n+\alpha} \right)^T = 0 \tag{67}$$

   This is nothing more than the previous scheme of section 3.2.4 applied between times t_n and $t_{n+\alpha}$. We get predicted states for $u_j^{n+\alpha}, j = 1, \cdots, n_s$.

2. Then we evaluate $u_j^{n+1}, j = 1, \cdots, n_s$ by solving

$$\sum_{T, M_i \in T} \left(\Phi^{K_2 *}_{j,n+\alpha} \right)^T + \sum_{T, M_i \in T} \left(\Phi^{K_2 *}_{j,n+1} \right)^T = 0 \tag{68}$$

In (67) and (68), the superscript T denotes the residuals relative to triangle T.

With this construction the resulting scheme is second order accurate both in time and space, and unconditionally monotone. Due to its non-linearity, equations (67) and (68) represent two systems of non-linear equations that we solve by Newton iterations. In the system case, we extend the scalar schemes to system schemes for both prisms K_1 and K_2 as described in sections 4.2.2 and 4.2.3. For example, the residual (52) is replaced by (41–42). Similar things are done for the relations (53) and (54) with obvious modifications.

5.1.3 Numerical example : Mach 3 Wind Tunnel with a Forward Facing Step

We use the same mesh of section 4.3.2, which is refined near the corner, with a fixed ratio $\Delta t_2 / \Delta t_1$ equal to 10. Isolines of density, Mach number and entropy at time $t = 4$ are shown. The density, Mach number and entropy deviation are shown on figures 18, 19 and 20. The results look very similar to those shown on Figure 11, 12 and 13. Hence, the same quality of results is obtained with an improved efficiency. This is very interesting in the case of very non uniform grids as here.

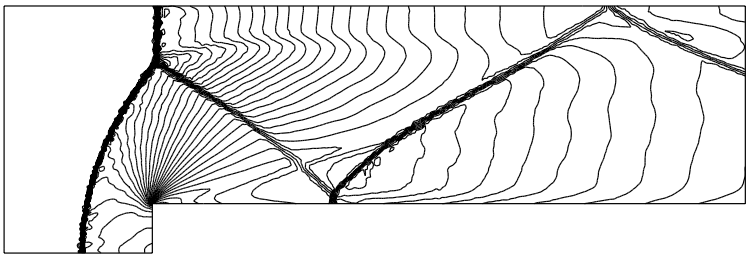

Figure 18: Forward-facing step problem. Density iso-lines: 30 equally spaced contour lines from 0.09 to 6.23. This has been computed with the unconditionally stable N-modified scheme.

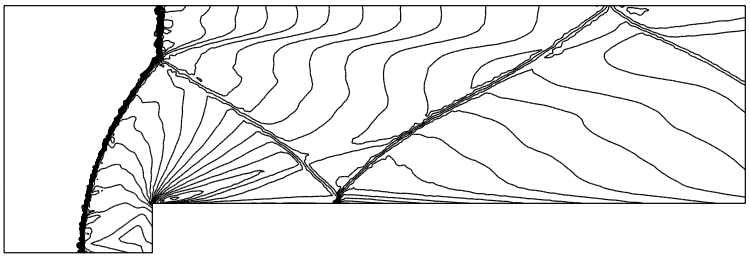

Figure 19: Forward-facing step problem. Mach number iso-lines: 25 equally spaced contour lines from 0.02 to 3.82. This has been computed with the unconditionally stable N-modified scheme.

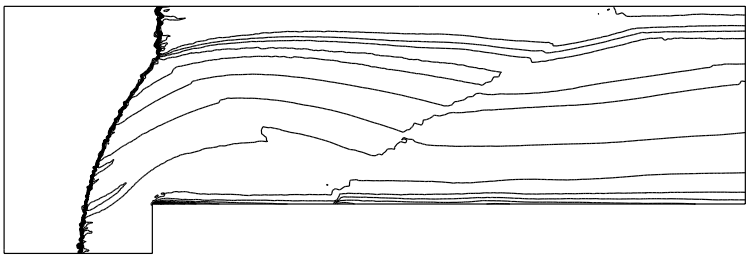

Figure 20: Forward-facing step problem. Entropy production near the step corner : 17 equally spaced contour lines from 0.63 to 1.5. This has been computed with the unconditionally stable N-modified scheme.

5.2 A single layer unconditionally monotone LP scheme

In this section we will present a single layer LP monotone scheme for which condition (27) can be relaxed. This is achieved by adopting, in the framework of the space-time schemes, the approach presented in [25] to construct very high order schemes for the solution of steady advection problems.

In [25] the authors consider the solution of the steady problem

$$\left\langle \overrightarrow{\lambda}, \nabla u \right\rangle = 0 \text{ in } \Omega \tag{69}$$

They show that a monotone formally k-th order accurate scheme can be constructed on an arbitrary triangulation τ_h of Ω starting from a first order linear monotone scheme. In particular, they consider schemes for which the discrete analog of (69) is of the form

$$\sum_{T, M_i \in T} \beta_i^T \Phi^T = 0$$

They prove that, provided that the distribution coefficients β_i^T are bounded, k-th order of accuracy is obtained if

$$\Phi^T = \int_T \left\langle \overrightarrow{\lambda}, \nabla u^h \right\rangle d\Omega = \mathcal{O}(h^{k+1})$$

Monotonicity is then guaranteed by defining the distribution coefficients such that for a given monotone scheme with distribution coefficients $(\beta_i^T)^{\mathrm{M}} = (\Phi_i^T)^{\mathrm{M}}/\Phi^T$ one has

$$\beta_i^T (\beta_i^T)^{\mathrm{M}} \geq 0$$

In [25] this is achieved through the use of definition (31) for the computation of the distribution parameters. The authors show that monotone and accurate results are obtained even if

$$\sum_{j \in T} (\Phi_j^T)^{\mathrm{M}} = \Phi^1 \neq \Phi^T ,$$

in particular they use always the first order N scheme (that is $\Phi^1 = \mathcal{O}(h^3)$) as the monotone scheme.

Here we will use a similar trick to obtain a non-linear scheme which inherits unconditional monotonicity from a first order unconditionally monotone scheme.

5.2.1 The unconditionally monotone "inconsistent" scheme

Consider the unsteady scalar problem. We start by defining a different version of the space-time N scheme. We first remark that (23) corresponds to the combination of the standard N scheme with Crank-Nicholson time integration for the inconsistent formulation (12). Our idea is to replace the Crank-Nicholson time integrator by an implicit Euler one. This yields, on a prismatic element $K = T \times [t_n, t_{n+1}]$, the following nodal residual

$$\Phi_{i,n+1} = \frac{|T|}{3}(u_i^{n+1} - u_i^n) + \Delta t \sum_{M_j \in T} k_i^+ N k_j^- (u_i^{n+1} - u_j^{n+1}) \tag{70}$$

Remark 5.1.

1. *scheme (70) verifies by construction the upwinding property:* $\Phi_{i,n} = 0 \, \forall i \in T$
2. *scheme (70) is not conservative with respect to the second order accurate element residual* Φ^T *given by (16):* $\sum_{j \in T} \Phi_{j,n+1} \neq \Phi^T$

Since the scheme verifies the upwinding property, we can simplify the notation and drop the sub-script $n+1$, so that, after assembling the contribution from all the elements, the scheme can be recast as

$$\sum_{T, M_i \in T} \Phi_i = 0$$

The scheme is of course implicit and can be recast as $Au^{n+1} = Bu^n$ with

$$A_{ii} = \sum_{T, M_i \in T} (\frac{|T|}{3} + \Delta t k_i^+) \quad , \quad A_{ij} = \sum_{T, (M_i, M_j) \in T} -\Delta t k_i^+ N k_j^- \tag{71}$$

$$B_{ii} = \sum_{T, M_i \in T} \frac{|T|}{3} \quad , \quad B_{ij} = 0. \tag{72}$$

The matrix B is diagonal with positive entries. The inverse of A always exists and has positive entries for all choices of the time step Δt. The scheme is then unconditionally monotone.

The extension to the Euler equations is obtained easily combining (52), (53) and (41).

5.2.2 A single layer unconditionally monotone and LP scheme

In order to get a consistent, conservative, monotone and second order accurate non-linear scheme, we proceed on each triangle T in τ_h as follows:

1. Compute the space-time fluctuation Φ^T according to (16)
2. $\forall j \in T$ compute the first order monotone residuals $(\Phi_j)^M$ according to (70)
3. $\forall j \in T$ compute the monotone distribution coefficients $(\beta_j)^M = (\Phi_j)^M / \Phi^T$
4. $\forall j \in T$ compute the bounded high order distribution coefficients β_j via (31)
5. $\forall j \in T$ compute Φ_j as $\Phi_j = \beta_j \Phi^T$

With this construction the resulting scheme is second order accurate both in time and space, and unconditionally monotone. We will present, for scalar and Euler problems, results confirming the unconditional stability of the scheme.

In the system case, we extend the scalar schemes to system schemes as described in sections 4.2.2 and 4.2.3.

5.2.3 Scalar Tests

The rotating cosine hill

We consider again the test case of the rotating cosine hill of section 3.3.1. The computational set-up is the same of section 3.3.1 except that here we investigate the influence on the quality of the solution of the magnitude of the time-step. In particular, we computed the time-step according to (27) and run this test case with the limited scheme described in the previous section and different values of the CFL number.

The results obtained after one revolution for values of the CFL equal to 0.9, 1.5, 3, 6, 9 and 12 are compared in figure 21. We provide the cross–sections at $y = 0$ in figure 22. We clearly see that the quality of the solution is little affected by the magnitude of the time-step up to $CFL = 6$. For CFL equal to 9 and 12 we start observing a degradation in the accuracy which is not surprising. In terms of height of the peak the results are very similar to the ones of section 3.3.1. We report the minimum and maximum values of the solution in table 2. We remark that monotonicity is preserved for all the values of the CFL number.

CFL	min	max
0.9	0	0.796
1.5	0	0.796
3.0	0	0.796
6.0	0	0.794
9.0	0	0.762
12.0	0	0.704

Table 2: Min and Max solution values for the rotating cosine hill test case.

The rotating cylinder

This is the same test of section 3.3.2. As in the previous section, we investigate here the influence of the time-step on the quality of the solution. As in the previous case we have run the simulation with different values of the CFL number, namely 0.9, 1.5, 3, 6, 9, and 12. The computation was made on the same grid. The results after one revolution are displayed in figure 23. Cross–sections of the solutions after one revolution are provided in figure 24. We see once more that

(i) The accuracy is is little affected by the time-step magnitude for CFL up to 6

(ii) Monotonicity is perfectly preserved for all the values of the CFL number

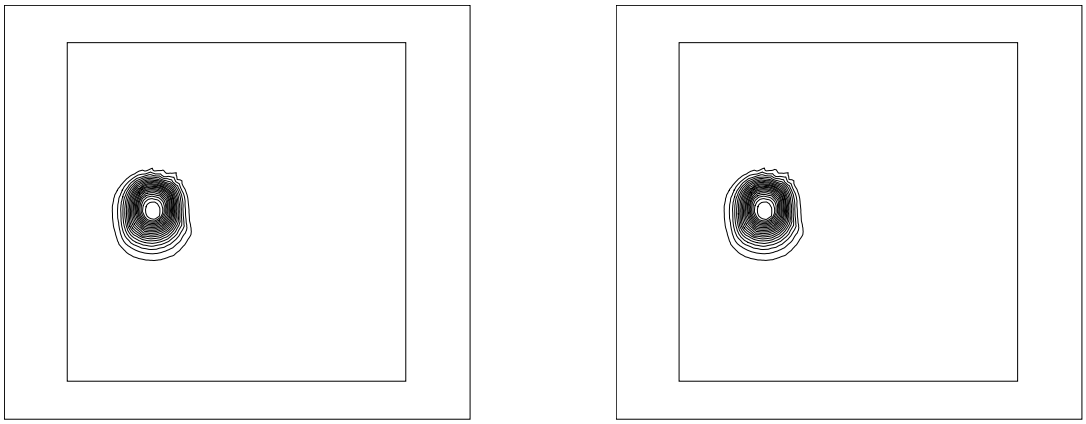

$CFL = 0.9$

$CFL = 1.5$

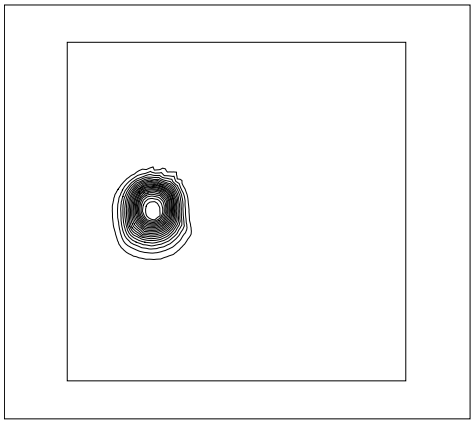

$CFL = 3.0$

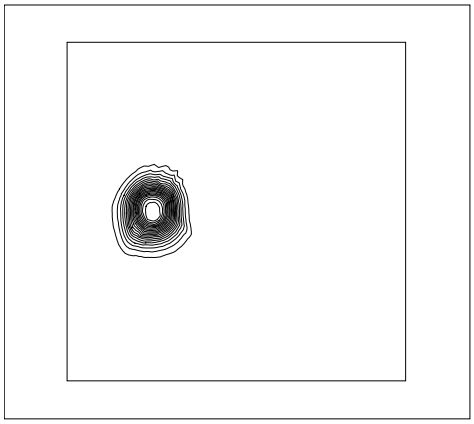

$CFL = 6.0$

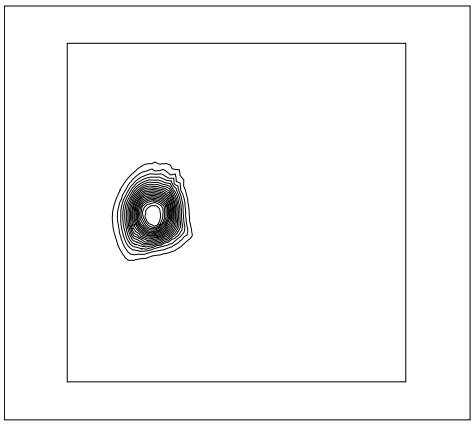

$CFL = 9.0$

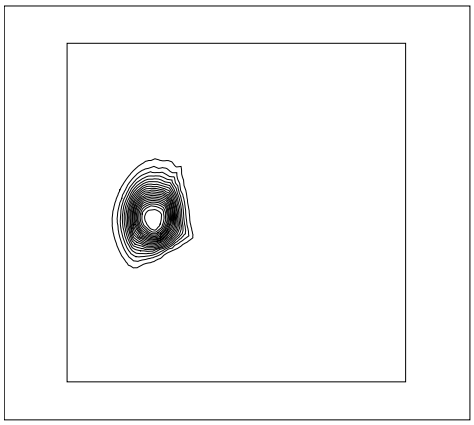

$CFL = 12.0$

Figure 21: Rotation of a cosine hill. Results with the unconditionally stable single layer N modified scheme for different CFL numbers. 20 contours of the solution

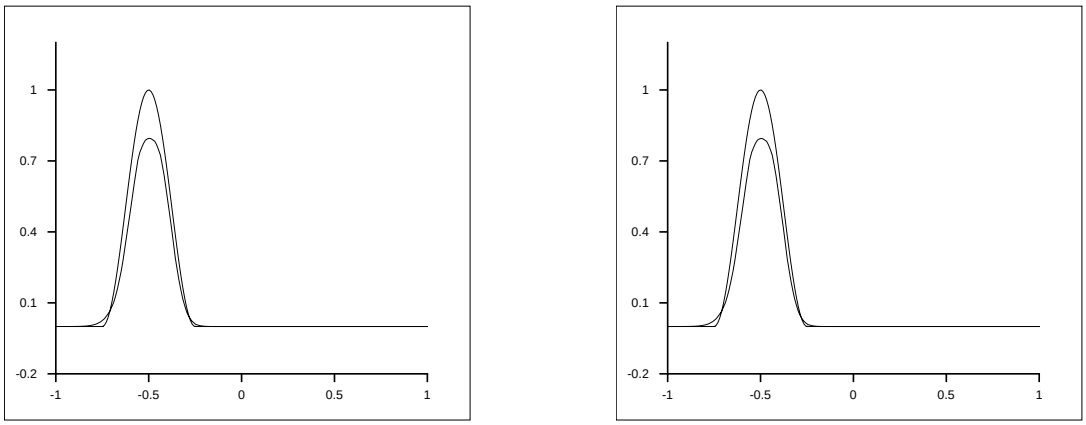

$CFL = 0.9$ $CFL = 1.5$

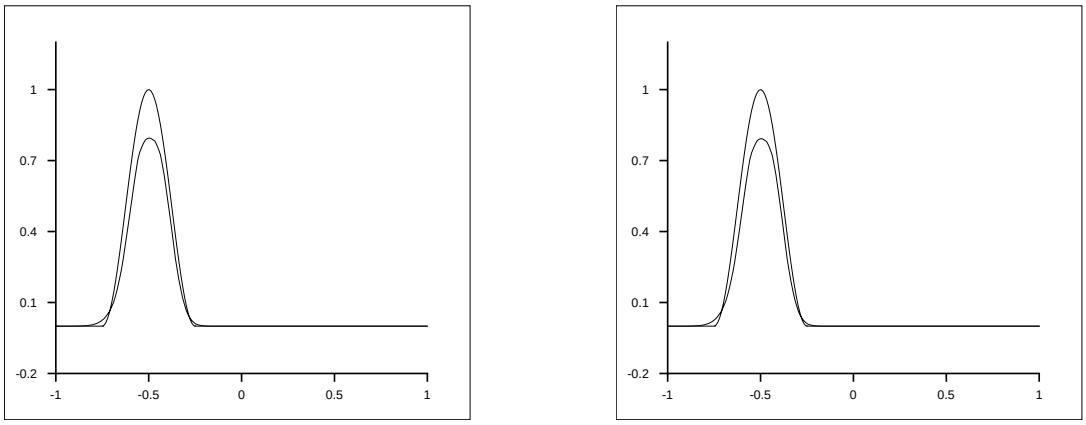

$CFL = 3.0$ $CFL = 6.0$

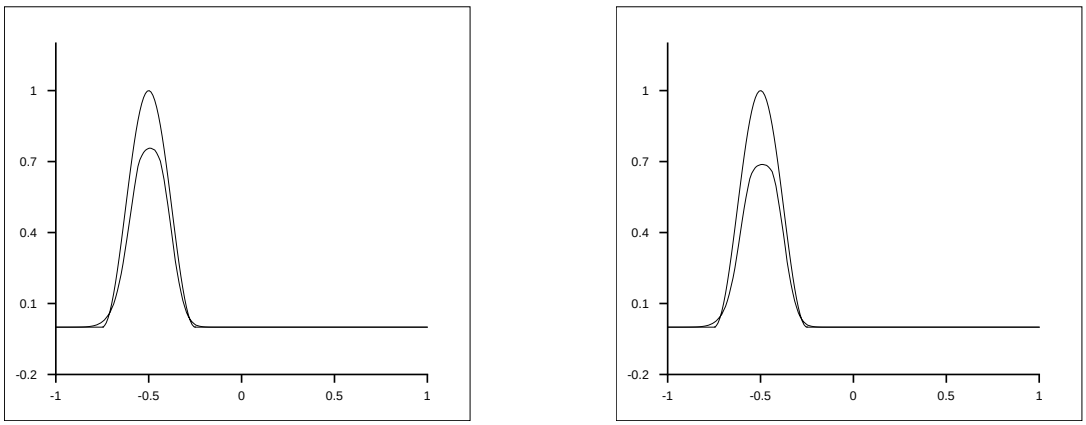

$CFL = 9.0$ $CFL = 12.0$

Figure 22: Rotation of a cosine hill. Results with the unconditionally stable single layer N modified scheme for different CFL numbers. Cut at $y = 0$

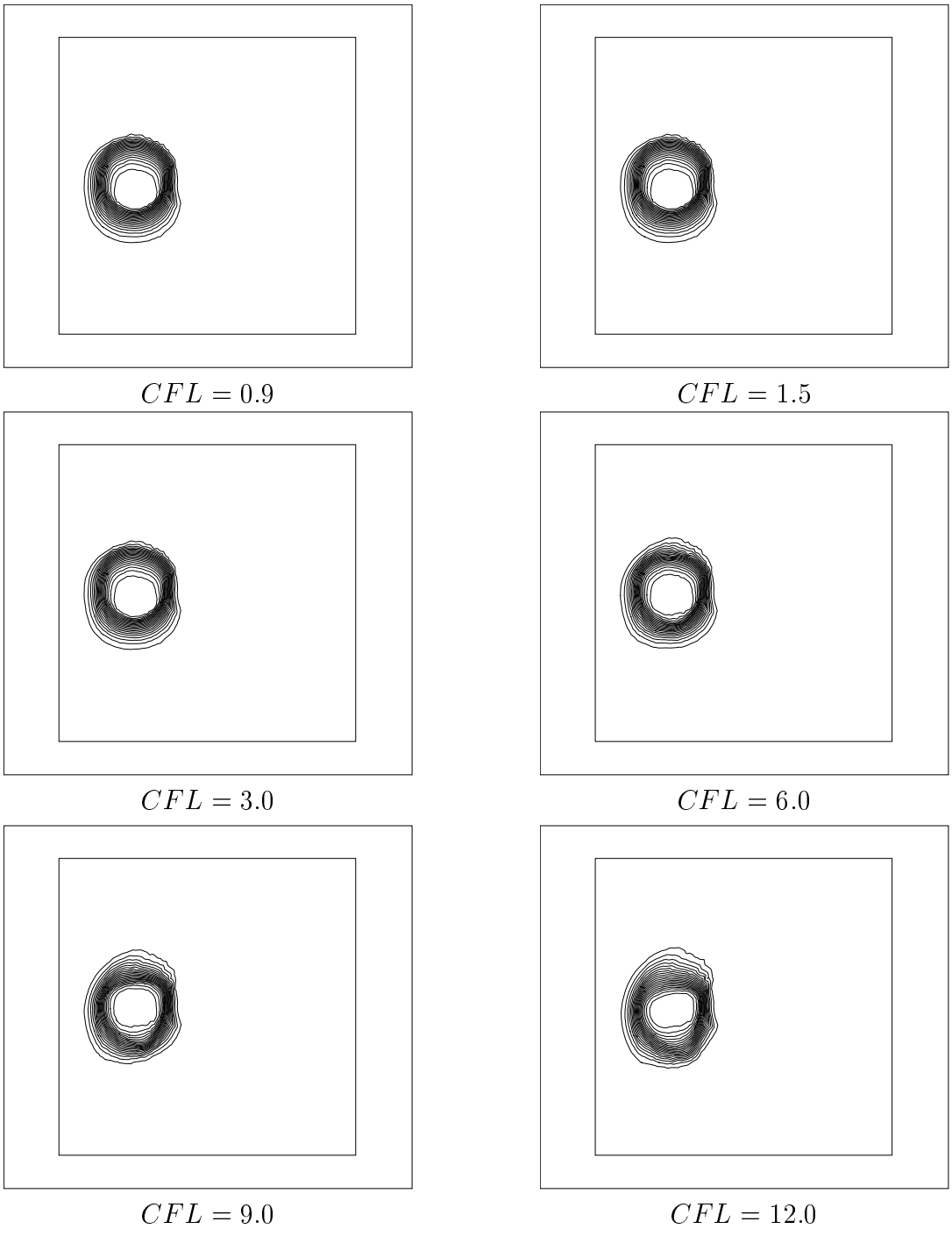

Figure 23: Rotation of a cylinder. Results with the unconditionally stable single layer N modified scheme for different CFL numbers. 20 contours of the solution

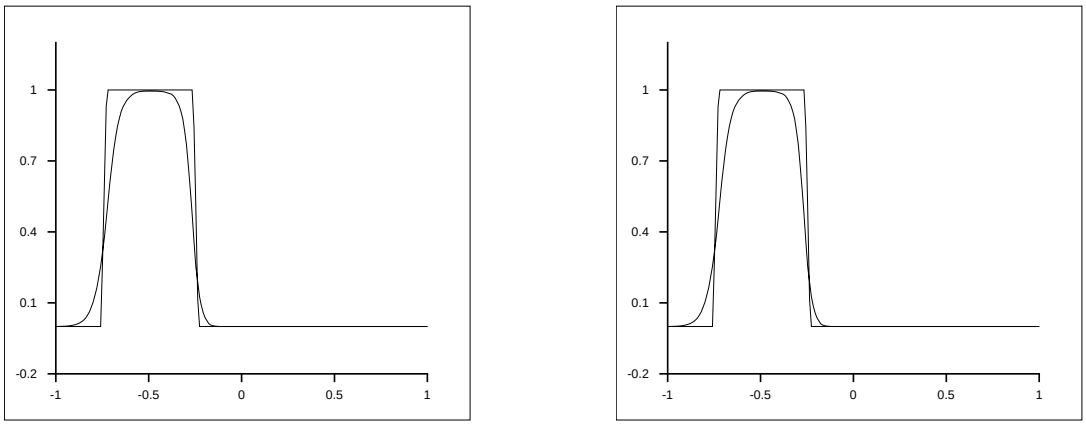

$CFL = 0.9$ $CFL = 1.5$

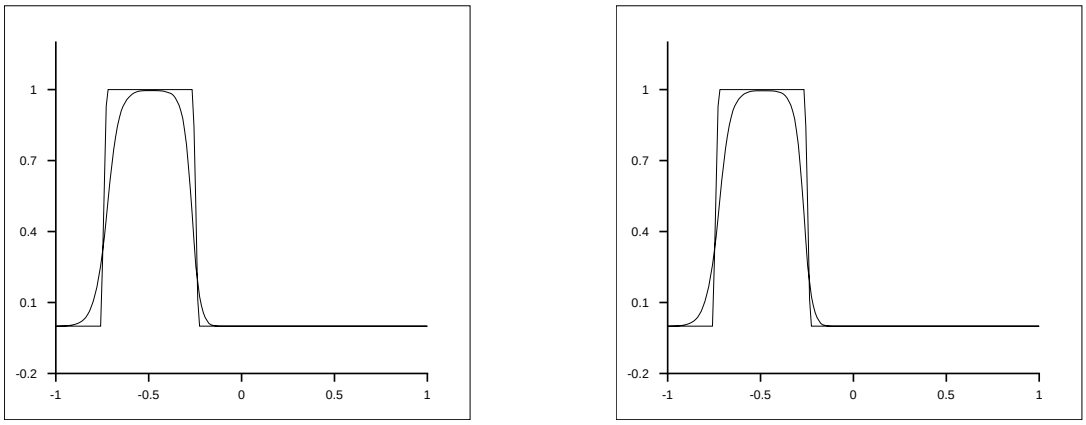

$CFL = 3.0$ $CFL = 6.0$

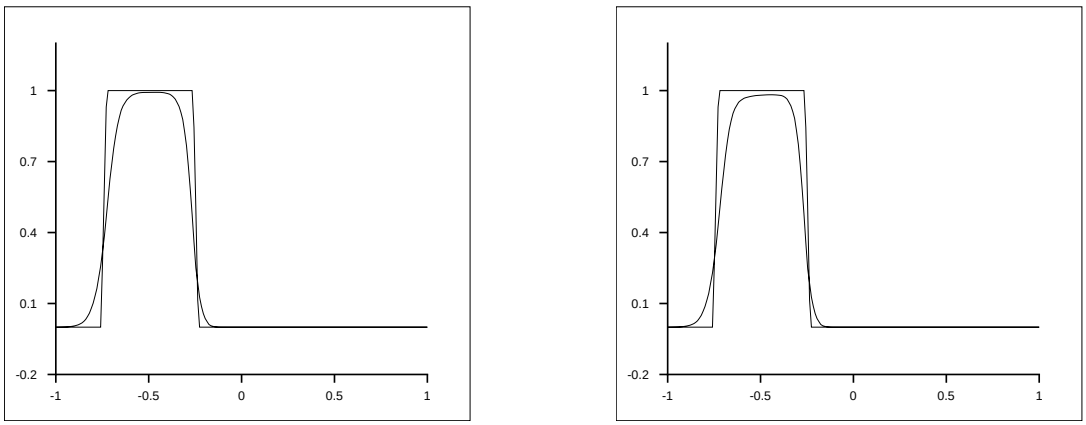

$CFL = 9.0$ $CFL = 12.0$

Figure 24: Rotation of a cylinder. Results with the unconditionally stable single layer N modified scheme for different CFL numbers. Cut at $y = 0$

5.2.4 Results for the Euler equations

A truly 2D Riemann problem

The first problem we consider is the two-dimensional Riemann problem presented already in [37, 38, 39]. The initial solution, sketched in figure 25, consists of four constant states describing the interaction between two oblique and two normal shocks moving upstream with respect to the flow velocity. The computational domain is $[0,1] \times [0,1]$. The initial solution is given by

$$(\rho, u, v, p) = \begin{cases} (1.5\ ,\ 0\ ,\ 0\ ,\ 1.5) & \text{if } x \geq 0.8 \text{ and } y \geq 0.8 \\ (0.5322581\ ,\ 1.2060454\ ,\ 0\ ,\ 0.3) & \text{if } x < 0.8 \text{ and } y \geq 0.8 \\ (0.1379928\ ,\ 1.2060454\ ,\ 1.2060454\ ,\ 0.0290323) & \text{if } x < 0.8 \text{ and } y < 0.8 \\ (0.5322581\ ,\ 0\ ,\ 1.2060454\ ,\ 0.3) & \text{if } x \geq 0.8 \text{ and } y < 0.8 \end{cases}$$

We have run this test with the system version of the modified N scheme presented in the last section. We have used this test to investigate the monotonicity of the scheme for increasing CFL numbers and its ability to resolve complex features of the solution in an accurate and monotone way.

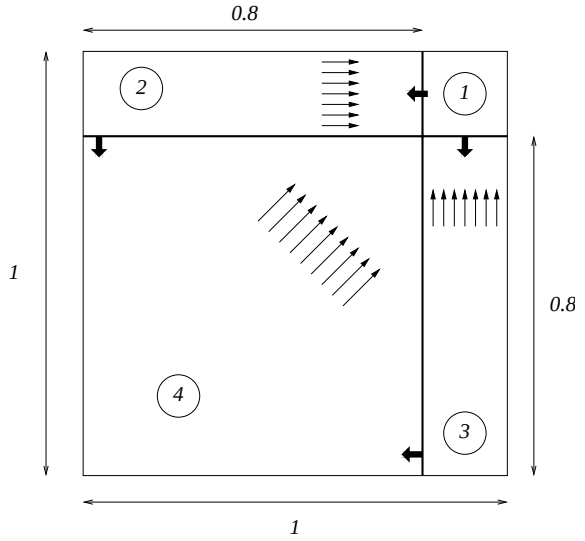

Figure 25: Initial solution and computational domain for the 2D Riemann problem

First we investigated the influence of the CFL number on the monotonicity of the scheme. We have solved the problem on an unstructured mesh containing 19928 triangles and 10166 nodes ($h \approx 1/100$). A zoom of the mesh is given in figure 26. The simulation was run for three different values of the CFL in (44), namely 1.5, 3.0 and 6.0. We display 25 density contours at time $t = 0.8$ in figures 26 and 27.

In all the figures we see that, even on such a coarse mesh, all the features of the solution are well resolved, especially the slip-lines originating from the triple points and the jet of fluid coming out of the initial singularity at $(x, y) = (0.8, 0.8)$. We can even see that, already on this mesh resolution, the slip lines show a mild instability. The most important remark is that, as in the scalar tests, the monotonicity of the scheme is not really affected from the increase in the CFL number. Moreover, the solutions for CFL 1.5 and 3.0 are very close in terms of accurate resolution of the interaction. On the other hand, the accuracy of the solution is clearly degraded in the case of $CFL = 6.0$.

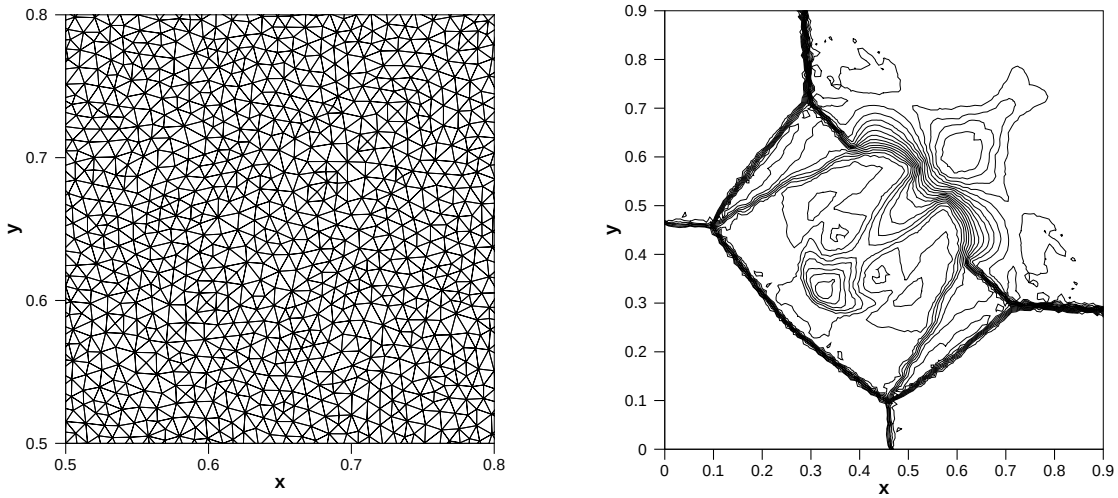

Figure 26: 2D Riemann Problem, $t = 0.8$. Left: mesh. Right: 25 density contours obtained with the unconditionally stable N modified system scheme and $CFL = 1.5$

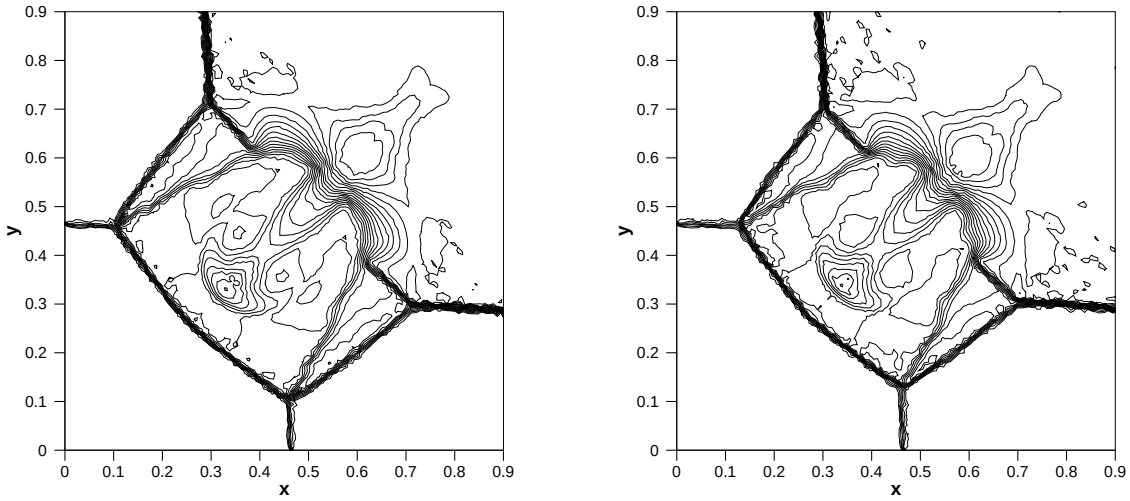

Figure 27: 2D Riemann Problem, $t = 0.8$. 25 density contours obtained with the unconditionally stable N modified system scheme. Left: $CFL = 3.0$ Right: $CFL = 6.0$

This can be especially seen in the resolution of the jet on the diagonal, which show clearly more dissipation. The inaccurate computation leads in this case to a wrong position of the shock normal to the diagonal.

In order to test the ability of the scheme to resolve very complex flow features, we computed a fine mesh solution of this problem. In [39] the authors have run this test with a time accurate Lax-Wendroff residual distribution scheme limited with an FCT procedure. They have computed this problem on regular triangular meshes obtained by subdividing the domain in quads and then cutting each quadrilateral with the right running diagonal. In the paper they show results on a very fine mesh obtained by subdividing each side of the domain in 400 segments. This gives, for their fine mesh, 320000 triangles and 160801 nodes. We have run this problem on an unstructured mesh like the one in figure 26 containing 316864 triangles and 159233 nodes ($h \approx 1/400$). We have run the simulation with $CFL = 1.5$. The results are displayed in figures 28, 29 and 30 where we show 25

contours of density, entropy ($s = p/\rho^\gamma$) and temperature ($T = p/\rho$) at time 0.8. We clearly see the ability of the scheme to resolve the complex instabilities of the flow in an accurate and monotone way. Compared to the results of [39], we see that our scheme shows less dissipation on the slip-lines coming out of the triple points, although in their solution the instabilities close to the fluid jet are better resolved.

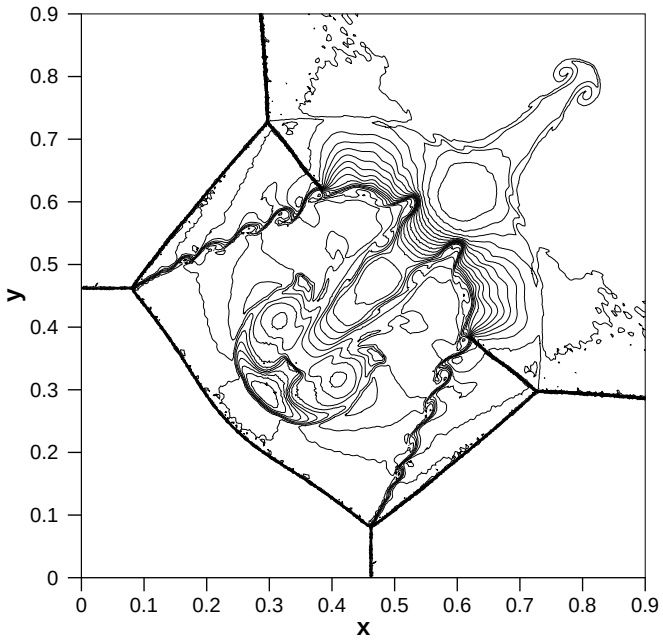

Figure 28: 2D Riemann Problem, $t = 0.8$. 25 density contours obtained on the fine mesh with the unconditionally stable N modified system scheme and $CFL = 1.5$

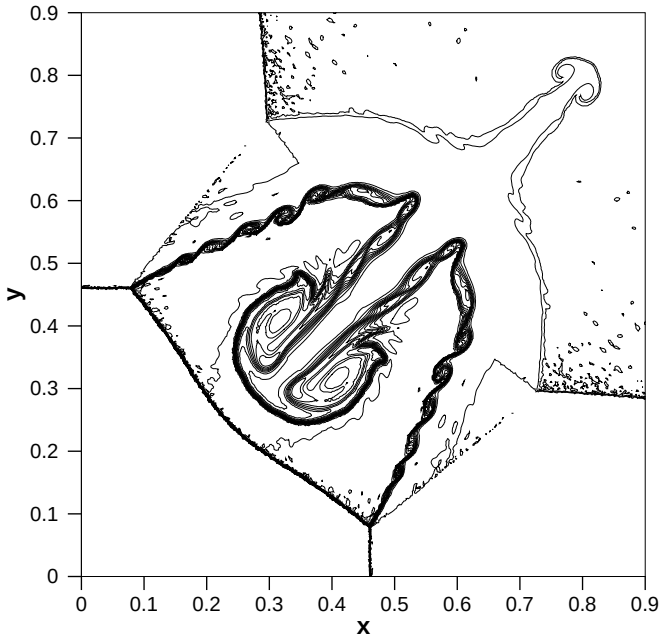

Figure 29: 2D Riemann Problem, $t = 0.8$. 25 entropy contours obtained on the fine mesh with the unconditionally stable N modified system scheme and $CFL = 1.5$

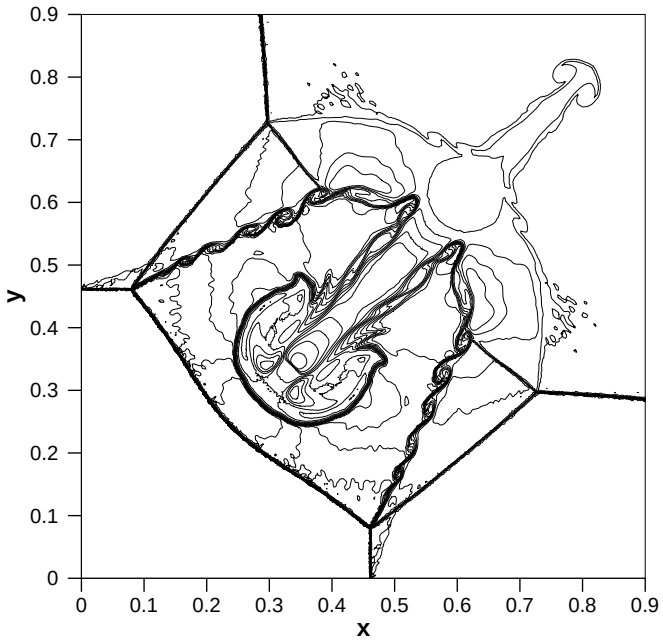

Figure 30: 2D Riemann Problem, $t = 0.8$. 25 temperature contours obtained on the fine mesh with the unconditionally stable N modified system scheme and $CFL = 1.5$

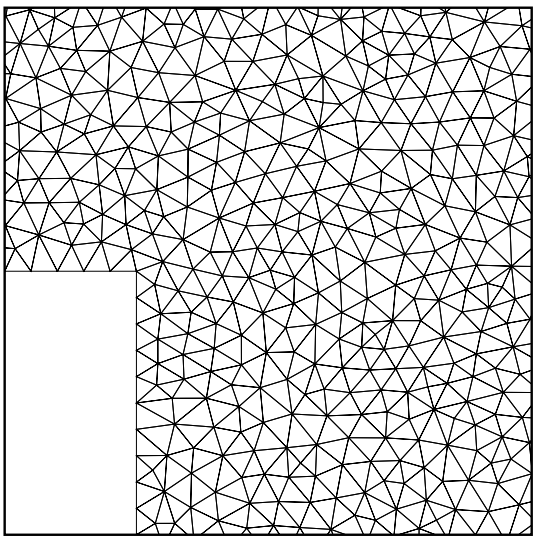

Figure 31: Shock diffraction problem: mesh close to the corner

The shock diffraction problem

This problem has been considered in [32]. It involves the diffraction of a shock wave on a 90° step. The computational domain is $([0,1] \times [6,11]) \bigcup ([1,13] \times [0,11])$. At time $t = 0$ a right moving Mach 5.09 shock wave is placed at $x = 0.5$. The gas ahead of the shock is stagnant and its pressure and density are taken to be 1 and 1.4 respectively. Inlet and outlet boundary conditions are applied at the left and right end of the domain, while reflective conditions are applied on the step. The corner of the step is a singularity of the problem . No special treatment has been applied in this point.

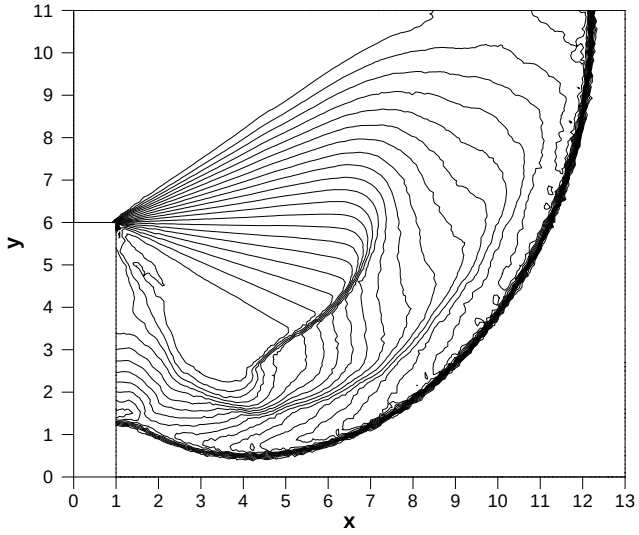

Figure 32: Shock diffraction problem, $t = 2.3$. 20 density contours

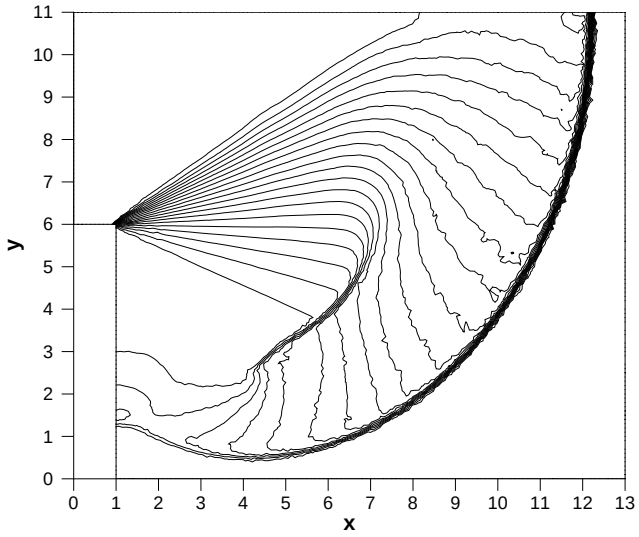

Figure 33: Shock diffraction problem, $t = 2.3$. 20 pressure contours

We solved the problem on a mesh containing 13869 nodes and 27256 triangles (reference mesh-size $h \approx 1/100$). A close-up view of the mesh in the vicinity of the corner is given in figure 31. The simulation has been run with the system version of the modified N scheme presented in the last section taking $CFL = 1.5$ in (44).

The results are presented in terms of density and pressure contours at time $t = 2.3$ in figures 32 and 33. The resolution of the secondary shock and of the slip-line are remarkable. We also underline that no negative density or pressure are present in the solution even if no ad-hoc treatment has been implemented for the singular point.

6 Comments on the efficiency

In the schemes we have presented, second order results can be obtained via a non linear Newton procedure. If first order results are sought, the scheme is also implicit with a linear implicit phase. How many iterations are needed to reach convergence or a satisfactory level of iterative residual ? Here, what we call the iterative residual is, in the scalar case, the maximum of the absolute values of the sum of residuals sent at node M_i. In other words, we are converged if for all M_i

$$\Big| \sum_{T, M_i \in T} \Phi_i \Big| \leq \epsilon$$

for the single layer monotone schemes and

$$\Big| \sum_{T, M_i \in T} \Phi^{K_1}_{i,n+\alpha} \Big| \leq \epsilon$$

and

$$\Big| \sum_{T, M_i \in T} \Phi^{K_2}_{i,n+\alpha} + \Phi i, n+1^{K_2} \Big| \leq \epsilon$$

for the unconditionally monotone two-layers scheme. The threshold is $\epsilon = 10^{-10}$ for the first order scheme and $\epsilon = 10^{-4}$ for the second order ones. The reason for these choices is that the first order scheme is energy stable so machine zero can be reached, while, as usual for Residual Distribution scheme, we do not know how to reach machine zero for high order non-linear schemes.

In all our experiments, we needed 3–4 Newton iterations to reached the prescribed level of iterative convergence.

7 Concluding remarks

We have developed a family of schemes for unsteady flow problems. The schemes are designed to work on truly unstructured triangular type meshes. The degrees of freedom are located at the vertices of the mesh. They use the most compact stencil for second order accuracy, namely the closest neighbors of a vertex. They are second order accurate in the sense that if the flow is smooth enough, the truncation error is $O(h^2)$, so that the error is formally second order even on irregular meshes. They are upwind, non oscillatory and parameter free. Lastly, it is possible to make them unconditionally stable without losing their basic properties (monotonicity, upwind and second order accurate).

A Energy-Stability of the Narrow scheme

This appendix contains the energy stability proof, *without any restriction on the time step* of the Narrow scheme for the symmetrizable system

$$\frac{\partial W}{\partial t} + \sum_{i=1}^{2} A_i \frac{\partial W}{\partial x_i} = 0 \quad (x,t) \in \mathbb{R}^2 \times \mathbb{R}^+, \tag{73}$$

where $W \in \mathbb{R}^m$ denotes the vector of conserved variables and the matrices A_i are assumed to be constant. Hence, we assume that there exists a symmetric positive definie matrix A_0 such that via the change of variables $W = A_0 V$, the system is

$$\widetilde{A}_0 \frac{\partial V}{\partial t} + \sum_{i=1}^{2} \widetilde{A}_i \frac{\partial V}{\partial x_i} = 0, \tag{74}$$

where $\widetilde{A}_0$ and the matrices $\widetilde{A}_i = A_i A_0$ are symmetric. The energy norm is defined by

$$\mathcal{E}(W)^2 = \frac{1}{2} \sum_T |T| \sum_{M_j \in T} \langle W_j, A_0 W_j \rangle.$$

In the following the notation $\widetilde{}$ over a matrix will mean that this matrix is symmetric.

The Narrow scheme reads

$$\sum_{T, M_i \in T} \left(\frac{|T|}{3}(W_i^{n+1} - W_i^n) + \frac{\Delta t}{2} \sum_{M_j \in T} K_i^+ N K_j^- (W_j^{n+1} - W_i^{n+1} + W_j^n - W_i^n) \right) = 0. \tag{75}$$

In symmetrization variables one has

$$\sum_{T, M_i \in T} \left(\frac{|T|}{3} \widetilde{A}_0 (V_i^{n+1} - V_i^n) + \frac{\Delta t}{2} \sum_{M_j \in T} \mathbf{K}_i^+ N \mathbf{K}_j^- (V_j^{n+1} - V_i^{n+1} + V_j^n - V_i^n) \right) = 0. \tag{76}$$

We first multiply this equation by $V_i^{n+1} + V_i^n$ to obtain

$$\begin{aligned} &\sum_{M_i \in T} \frac{|T|}{3} \langle \widetilde{A}_0 (V_i^{n+1} - V_i^n), V_i^{n+1} + V_i^n \rangle \\ &+ \frac{\Delta t}{2} \sum_{T, M_i \in T} \sum_{M_j \in T} \langle \mathbf{K}_i^+ N \mathbf{K}_j^- (V_j^{n+1} - V_i^{n+1} + V_j^n - V_i^n), V_i^{n+1} + V_i^n \rangle = 0 \end{aligned} \tag{77}$$

Summing over the nodes of the mesh we get

$$\begin{aligned} &\sum_{T \in \tau_h} \left(\sum_{M_i \in T} \frac{|T|}{3} \langle \widetilde{A}_0 (V_i^{n+1} - V_i^n), V_i^{n+1} + V_i^n \rangle \right. \\ &\left. + \frac{\Delta t}{2} \sum_{M_i \in T} \sum_{M_j \in T} \langle \mathbf{K}_i^+ N \mathbf{K}_j^- (V_j^{n+1} - V_i^{n+1} + V_j^n - V_i^n), V_i^{n+1} + V_i^n \rangle \right) = 0 \end{aligned} \tag{78}$$

Using the fact that $\widetilde{A}_0$ is symmetric, one has

$$\begin{aligned} \langle \widetilde{A}_0 (V_i^{n+1} - V_i^n), V_i^{n+1} + V_i^n \rangle &= \langle \widetilde{A}_0 V_i^{n+1}, V_i^{n+1} \rangle + \langle \widetilde{A}_0 V_i^{n+1}, V_i^n \rangle \\ &- \langle \widetilde{A}_0 V_i^n, V_i^n \rangle - \langle \widetilde{A}_0 V_i^n, V_i^{n+1} \rangle \\ &= \langle \widetilde{A}_0 V_i^{n+1}, V_i^{n+1} \rangle - \langle \widetilde{A}_0 V_i^n, V_i^n \rangle \end{aligned}$$

The second term of (78) can be written as

$$\begin{aligned}
&\sum_{M_i\in T}\Big(\sum_{M_j\in T}\langle \mathbf{K}_i^+ N\mathbf{K}_j^-(V_j^{n+1}-V_i^{n+1}+V_j^n-V_i^n),V_i^{n+1}+V_i^n\rangle\Big) = \\
&\qquad \sum_{M_i\in T}\Big(\sum_{M_j\in T}\langle \mathbf{K}_i^+ N\mathbf{K}_j^-(V_j^{n+1}+V_j^n),V_i^{n+1}+V_i^n\rangle \\
&\qquad\qquad -\sum_{M_j\in T}\langle \mathbf{K}_i^+ N\mathbf{K}_j^-(V_i^{n+1}+V_i^n),V_i^{n+1}+V_i^n\rangle\Big) \\
&+\sum_{M_i\in T}\Big(\sum_{M_j\neq M_i}\langle \mathbf{K}_i^+ N\mathbf{K}_j^-(V_j^{n+1}+V_j^n),V_i^{n+1}+V_i^n\rangle + \langle \mathbf{K}_i^+(V_i^{n+1}+V_i^n),V_i^{n+1}+V_i^n\rangle\Big)
\end{aligned}$$

In equation (78) we can add the term $-\sum_{T\in\tau_h}\sum_{i\in T}\langle \mathbf{K}_i(V_i^{n+1}+V_i^n),V_i^{n+1}+V_i^n\rangle$ because this term is equal to zero since the geometry surrounding a vertex is closed.

$$\begin{aligned}
\sum_{T\in\tau_h}\sum_{M_i\in T}\langle \mathbf{K}_i(V_i^{n+1}+V_i^n),V_i^{n+1}+V_i^n\rangle &= \sum_{M_i\in\tau_h}\sum_{T,M_i\in T}\langle \mathbf{K}_i(V_i^{n+1}+V_i^n),V_i^{n+1}+V_i^n\rangle \\
&= \sum_{M_i\in\tau_h}\Big\langle\big(\sum_{T,M_i\in T}\mathbf{K}_i\big)(V_i^{n+1}+V_i^n),V_i^{n+1}+V_i^n\Big\rangle \\
&= 0
\end{aligned}$$

Equation (78) becomes

$$\begin{aligned}
&\sum_{T\in\tau_h}\sum_{M_i\in T}\frac{|T|}{3}(\langle \widetilde{A}_0V_i^{n+1},V_i^{n+1}\rangle-\langle \widetilde{A}_0V_i^n,V_i^n\rangle) \\
&+\frac{\Delta t}{2}\sum_{T\in\tau_h}\sum_{M_i\in T}\Big(\frac{1}{2}\langle|\mathbf{K}_i|(V_i^{n+1}+V_i^n),V_i^{n+1}+V_i^n\rangle \\
&\qquad +\sum_{M_j\in T}\langle \mathbf{K}_i^+ N\mathbf{K}_j^-(V_j^{n+1}+V_j^n),V_i^{n+1}+V_i^n\rangle\Big) = 0
\end{aligned} \tag{79}$$

Moreover one has

$$\begin{aligned}
\sum_{M_i\in T}\sum_{M_j\in T}\langle \mathbf{K}_i^+ N\mathbf{K}_j^-(V_j^{n+1}+V_j^n),V_i^{n+1}+V_i^n\rangle &= \sum_{M_i\in T}\sum_{M_j\in T}\langle V_j^{n+1}+V_j^n,\mathbf{K}_j^- N\mathbf{K}_i^+(V_i^{n+1}+V_i^n)\rangle \\
&= \sum_{M_j\in T}\sum_{M_i\in T}\langle \mathbf{K}_j^- N\mathbf{K}_i^+(V_i^{n+1}+V_i^n),V_j^{n+1}+V_j^n\rangle
\end{aligned}$$

Equation (79) becomes

$$\sum_{T\in\tau_h}\sum_{M_i\in T}\frac{|T|}{3}(\langle\widetilde{A}_0V_i^{n+1},V_i^{n+1}\rangle-\langle\widetilde{A}_0V_i^{n},V_i^{n}\rangle)$$

$$+\frac{\Delta t}{2}\sum_{T\in\tau_h}\sum_{M_i\in T}\left(\frac{1}{2}\langle|\mathbf{K}_i|(V_i^{n+1}+V_i^n),V_i^{n+1}+V_i^n\rangle\right.$$

$$+\sum_{M_j\in T}\frac{1}{2}\langle\mathbf{K}_i^+N\mathbf{K}_j^-(V_j^{n+1}+V_j^n),V_i^{n+1}+V_i^n\rangle+ \tag{80}$$

$$\left.\frac{1}{2}\langle\mathbf{K}_i^-N\mathbf{K}_j^+(V_j^{n+1}+V_j^n),V_i^{n+1}+V_i^n\rangle\right)=0$$

Next, rewrite

$$\mathbf{K}_i^+N\mathbf{K}_j^-+\mathbf{K}_i^-N\mathbf{K}_j^+$$

in the following form

$$K_i^+N\mathbf{K}_j^-+\mathbf{K}_i^-N\mathbf{K}_j^+=\mathbf{K}_iN\mathbf{K}_j+\mathbf{K}_i^+N\mathbf{K}_j^++\mathbf{K}_i^-N\mathbf{K}_j^-,$$

which leads to

$$0=\sum_{T\in\tau_h}\sum_{M_i\in T}\frac{|T|}{3}(\langle\widetilde{A}_0V_i^{n+1},V_i^{n+1}\rangle-\langle\widetilde{A}_0V_i^{n},V_i^{n}\rangle)$$

$$+\frac{\Delta t}{2}\sum_{T\in\tau_h}\sum_{M_i\in T}\left(\frac{1}{2}\langle\mathbf{K}_iN\mathbf{K}_j(V_j^{n+1}+V_j^n),V_i^{n+1}+V_i^n\rangle\right.$$

$$+\frac{1}{2}\langle\mathbf{K}_i^+(V_i^{n+1}+V_i^n),V_i^{n+1}+V_i^n\rangle-\frac{1}{2}\sum_{M_j\in T}\langle\mathbf{K}_i^+N\mathbf{K}_j^+(V_j^{n+1}+V_j^n),V_i^{n+1}+V_i^n\rangle \tag{81}$$

$$\left.+\frac{1}{2}\langle-\mathbf{K}_i^-(V_i^{n+1}+V_i^n),V_i^{n+1}+V_i^n\rangle+\frac{1}{2}\sum_{M_j\in T}\langle\mathbf{K}_i^-N\mathbf{K}_j^-(V_j^{n+1}+V_j^n),V_i^{n+1}+V_i^n\rangle\right)$$

Finally one obtains

$$\sum_{T\in\tau_h}\sum_{M_i\in T}\frac{|T|}{3}(\langle\widetilde{A}_0V_i^{n+1},V_i^{n+1}\rangle-\langle\widetilde{A}_0V_i^{n},V_i^{n}\rangle)$$

$$+\sum_{T\in\tau_h}\left(Q_a^T(V_1,V_2,V_3)+Q_b^T(V_1,V_2,V_3)+Q_c^T(V_1,V_2,V_3)\right)=0 \tag{82}$$

In [40], it is shown that Q_a^T, Q_b^T and Q_c^T are positive quadratic forms : the system N scheme is energy stable.

References

[1] E. Godlewski and P.A. Raviart. *Hyperbolic systems of conservations laws, I.* Ellipse, 1991.

[2] E. Godlewski and P.A. Raviart. *Hyperbolic systems of conservations laws.* Applied Mathematical Sciences. Springer Verlag, 1995.

[3] L. Fezoui and B. Stoufflet. A class of implicit upwind schemes for Euler simulations with unstructured meshes. *J. Comput. Phys.*, 84(1):174–206, 1989.

[4] C. Johnson, U. Nvert, and J. Pitkranta. Finite element methods for linear hyperbolic problems. *Computer methods in applied mechanics and engineering*, pages 285–312, 1984.

[5] Th.J.R. Hughes and M. Mallet. A new finite element formulation for Computational Fluid Dynamics : III the generalized streamline operator for multidimensional advective–diffusive systems. *Computer Methods in Applied Mechanics and Engineering*, 58:305–328, 1986.

[6] B. Cockburn and C.-W. Shu. The local discontinuous Galerkin method for time-dependent convection-diffusion systems. *SIAM J. Numer. Anal.*, 35(6):2440–2463 (electronic), 1998.

[7] A. Harten, S. Osher, B. Engquist, and S.R. Chakravarthy. Uniformly high–order accurate non–oscillatory schemes iii. *J. Comput. Phys.*, 71:231–303, 1987.

[8] C. Hu and C.W. Shu. Weighted essentially non-oscillatory schemes on triangular meshes. *J. Comput. Phys.*, 150(1):97–127, 1999.

[9] R. Abgrall. On Essentially Non-Oscillatory Schemes on Unstructured Meshes : Analysis and Implementation. *J. Comp. Phys.*, 114(1):45–54, September 1994.

[10] O. Friedrich. Weighted essentially non-oscillatory schemes for the interpolation of mean values on unstructured grids. *J. Comput. Phys.*, 144(1):194–212, 1998.

[11] Th.J.R. Hughes and M. Mallet. A new finite element formulation for Computational Fluid Dynamics : IV a discontinuity–capturing operator for multidimensional advective–diffusive systems. *Computer Methods in Applied Mechanics and Engineering*, 58:329–336, 1986.

[12] M.Y. Hussaini, B. van Leer, and J. Van Rosendal, editors. *Upwind and High Resolution Schemes.* Springer Verlag, 1997.

[13] R. Struijs, H. Deconinck, and P. L. Roe. Fluctuation Splitting Schemes for the 2D Euler equations. *VKI LS 1991-01, Computational Fluid Dynamics*, 1991.

[14] H. Deconinck, R. Struijs, G. Bourgeois, and P.L. Roe. Compact advection schemes on unstructured meshes. VKI Lecture Series 1993–04, Computational Fluid Dynamics, 1993.

[15] P.L. Roe and D. Sidilkover. Optimum positive linear schemes for advection in two and three dimensions. *Siam J. Numer. Anal.*, 29(6):1542–1588, 1992.

[16] E. van der Weide and H. Deconinck. Positive matrix distribution schemes for hyperbolic systems. In *Computational Fluid Dynamics '96*, pages 747–753. Wiley, 1996.

[17] R. Abgrall. Toward the ultimate conservative scheme: following the quest. *J. Comput. Phys.*, 167(2):277–315, 2001.

[18] R. Abgrall and T. Barth. Weighted residual distribution schemes for conservation laws via adaptive quadrature. *Siam J. Sci. Comput.*, 2002. in press.

[19] R. Abgrall and M. Mezine. A consistent upwind residual scheme for scalar unsteady advection problem s. Conference AMIF organized by the European Science Foundation, Tuscany, Italy, October 2000.

[20] A. Ferrante. Solution of the unsteady euler equations using residual distribution and flux correcte transport. Technical report, von Kàrman Institute, Chaussée de Waterloo, 72, B-1640 Rhode Saint Genèse, Belgium, 1997. Project report.

[21] M. Hubbard and P.L. Roe. Compact high resolution algorithms for time dependent advection problems on unstructured grids. *Int. J. Numer. Methods Fluids*, 33(5):711–736, 2000.

[22] D. Caraeni and L. Fuchs. Compact third–order multidimensional upwind scheme for navier stokes simulations. *Theoretical and Computational Fluid Dynamics*, 15(2):373–401, 2002.

[23] À Csik, M. Ricchiuto, H. Deconinck, and S. Poedts. Space–time residual distribution schemes for hyperbolic conservation laws. AIAA 2001–2617, 15th AIAA Computational Fluid Dynamics Conference, Anahein, CA, USA, June 2001.

[24] R. Abgrall and M. Mezine. Construction of second order accurate monotone and stable residual schemes : the steady case. *JCP*, 2002. soumis, http://www.math.u-bordeaux/∼abgrall/Articles/steady.ps.gz.

[25] R. Abgrall and P.L. Roe. Construction of very high order fluctuation scheme. *J. Scientific Computing*, 2003. in press, http://www.math.u-bordeaux/∼abgrall/Articles/high.ps.gz.

[26] H. Deconinck, R. Struijs, G. Bourgeois, and P.L. Roe. Compact advection schemes on unstructured meshes. VKI Lecture Series 1993–04, Computational Fluid Dynamics, 1993.

[27] H. Deconinck, K. Sermeus, and R. Abgrall. Status of multidimensional upwind residual distribution schemes and applications in aeronautics. AIAA paper 2000-2328, June 2000. AIAA CFD Conference, Denver (USA).

[28] P. Lascaux and R. Théodor. *Analyse numérique matricielle appliquée à l'art de l'ingénieur*. Masson, Paris, France, 1986.

[29] Árpád György Csík. *Upwind Residual Distribution Schemes for General Hyperbolic Conservation Laws and Application to Ideal Magnetohydrodynamics*. PhD thesis, Katholieke Universiteit Leuven, Faculteit Wetenschappen Centrum voor Plasma-Astrofysica, Belgium, Oct 2002.

[30] R. Struijs, H. Deconinck, and P.L. Roe. Fluctuation splitting schemes for the 2d euler equations. VKI LS 1991-01, 1991. Computational Fluid Dynamics.

[31] P. Collela and P. Woodward. The numerical simulation of two-dimensionnal fluid with strong shocks. *J. Comput. Phys.*, 54:115–173, 1984.

[32] J.J. Quirk. A contribution to the great riemann solver debate. *Int. J. Numer. Methods Fluids*, 18(555-574), 1994.

[33] G. Ben-Dor. *Shock Wave Reflection Phenomena*. Springer–Verlag, Berlin/New York, 1991.

[34] S. P. Pao and M. D. Salas. AIAA Paper 81-1205, 1981.

[35] K. R. Meadows, A. Kumar, , and M. Y. Hussaini. A computational study of the interaction between a vortex and a shock wave. AIAA Paper 89-1043, 1989.

[36] G.-S. Jiang and C.-W. Shu. Efficient implementation of weighted eno schemes. *J. Comput. Phys.*, 126:202–228, 1996.

[37] J.P. Collins C.W. Schults-Rinne and H.M. Glaz. Numerical solution of the riemann problem for two-dimensional gas dynamics. *SIAM J. Numer. Anal.*, 14, 1993.

[38] R.J. Le Veque. Wave propagation algorithms for multidimensional hyperbolic systems. *J. Comput. Phys.*, 131:327–353, 1997.

[39] G. Pascazio P. De Palma and M. Napolitano. An accurate fluctuation splitting scheme for the unsteady two-dimensional euler equations. ECCOMAS CFD Conference, 2001, Swansea, Wales, UK, September 2001.

[40] R. Abgrall, K. Mer, and B. Nkonga. A lax–wendroff type theorem for residual schemes. In M. Haffez and J.J Chattot, editors, *Innovative methods for numerical solutions of partial differential equations*, pages 243–266. World Scientific, 2002.